

# **Trapping of Non-Aqueous Phase Liquids at Sand/Shale Interfaces**

By:

Claire Chia-lan Hsu

Submitted in partial Fulfillment of the Requirements  
for the Degree of Master of Science in Hydrology

New Mexico Institute of Mining and Technology  
Department of Earth and Environmental Sciences

Socorro, New Mexico

April, 1998

## ABSTRACT

Spilled nonaqueous phase liquids (NAPLs) can be trapped by relatively small-scale structures at sand/shale interfaces just as hydrocarbons are naturally trapped in larger scale structures in oil and gas fields. When NAPLs are immobilized by trapping at sand/shale interfaces they may become a long-term source of contamination because conventional pump and treat remediation methods may not adequately remove them. At the same time, NAPLs immobilized at sand/shale interfaces can only have a limited effect on the aquifer because dispersion and dilution processes will act over some finite distance to decrease dissolved NAPL concentrations below regulatory limits. Micro-scale closure, defined as the height of the trapping feature, was measured on the upper sand surface immediately below the overlying shale for 62 locations at three sites for fluvial/alluvial and tidal flat depositional environments. Closure volume ranged from a low of 0.56 L/m<sup>2</sup> to a high of 2.88 L/m<sup>2</sup>. The average for all sites was 1.22 L/m<sup>2</sup>. The area of each measurement ranged between 1024 and 2090 cm<sup>2</sup>. Closure height of the sites could not be measured for individual features, so topographic variation was measured at each of the 62 locations. Topographic variation ranged up to a maximum of 3.3 cm, and site means ranged between 1.3 and 2.4 cm.

Sand-box experiments were also conducted to see if micro-scale features have NAPL trapping potential. The results suggest that for NAPL's to be trapped at greater than residual saturation, the trap closure height must be greater than the capillary rise of water into the NAPL. A closure of 4.0 cm effectively trapped Marvel Mystery Oil™ when the average grain size was 1.5 mm, but failed to do so at smaller grain-sizes. The experimental results are adequately reproduced by Hobson's Formula which states that

the height of capillary rise is inversely proportional to grain-size and is also a function of the physical properties of the NAPL. Further calculations using Hobson's Formula suggest that traps containing coarse-grained material are effective for some NAPLs at closures approaching one cm, while fine-grained sands required minimum closures of slightly less than one meter to five meters or more to trap NAPLs.

## ACKNOWLEDGEMENTS

The Waste-education Management and Research Consortium and the New Mexico Bureau of Mines and Mineral Resources supported this research.

Thanks to Dr. Fred Philips, Dr. Brian McPherson, and Dr. Peter Mozley for being on my committee and for their time and advice. I thank Dr. Mike Whitworth for his guidance and assistance on the direction of the research and help with field work. I also want to thank Dr. Stephen Schery, Maqsood Ali, Dennis Romero, John Sigda for many useful discussions, Bill DeMarco for his help with the photography for the visualization experiments, Fred Yarger and Roy Dixon for proof-reading this document, and Magsood Ali, Dennis Romero, Sung Ho Hong, and Paul Lecher for their help in the field.

I wish to acknowledge my family and friends for their support through my work. Most of all, thanks are due to my husband, Roy Dixon, for his support.

## TABLE OF CONTENTS

<b>CHAPTER 1 - INTRODUCTION .....</b>	<b>(1)</b>
<b>CHAPTER 2 – FIELD WORK.....</b>	<b>(5)</b>
Site Geology ... ..	(5)
Methods ... ..	(14)
Results ... ..	(16)
<b>CHAPTER 3 – SAND BOX EXPERIMENTS.....</b>	<b>(20)</b>
Previous Work .....	(20)
Material, Apparatus, and Procedure.....	(20)
Results.....	(23)
<b>CHAPTER 4 – THE ROLE OF CAPILLARY FORCES IN NAPL TRAPPING:</b>	
<b>A CONCEPTUAL MODEL.....</b>	<b>(34)</b>
<b>CHAPTER 5 – DISCUSSION.....</b>	<b>(38)</b>
<b>CHAPTER 6 - SUMMARY AND CONCLUSIONS .....</b>	<b>(48)</b>
<b>REFERENCES CITED .....</b>	<b>(51)</b>
<b>APPENDIX A – SITE INFORMATION.....</b>	<b>(53)</b>
<b>APPENDIX B - SAND/SHALE INTERFACE CLOSURE DATA .....</b>	<b>(54)</b>
<b>APPENDIX C – ELEVATION MEASUREMENTS.....</b>	<b>(66)</b>

## LIST OF FIGURES

FIGURE	PAGE
1. Measured section from Site 1 showing location of excavated sandstone surface .....	(6)
2. Photograph of excavated sandstone surface at surface at Site 1 .....	(8)
3. Measured section from Site 2 showing location of excavated surface. ....	(9)
4. Photograph of the excavated upper sand surface at Site 2.....	(10)
5. Measured section from Site 3 showing location of excavated sandstone surface ....	(12)
6. Photograph of excavated sandstone surface at Site 3 .....	(13)
7. Site 1 closure volume versus frame size for Site 1 .....	(18)
8. Closure volume for frame size 1024 cm <sup>2</sup> for all sites .....	(19)
9. Schematic of sandbox used in NAPL visualization Experiments.....	(22)
10. Results of sand box visualization experiment 1 .....	(25)
11. Results of sand box visualization experiment 2.....	(28)
12. Results of sand box visualization experiment 3.....	(31)
13. Results of sand box visualization experiment 4.....	(33)
14. Definition of contact angle $\theta$ (modified from Fetter, 1993) .....	(35)
15. Relation of height of capillary rise of water in to benzene versus grain-size of aquifer matrix .....	(40)
16. Relation of height of capillary rise of water in to diesel fuel versus grain-size of aquifer matrix.....	(41)
17. Relation of height of capillary rise of water in to dichloromethane versus grain-size of aquifer matrix.....	(43)
18. Relation of height of capillary rise of water in to trichloromethane versus grain-size of aquifer matrix .....	(44)

## LIST OF TABLES

TABLE	PAGE
1. Site 1 summary data.....	(17)
2. Summary data for different sites with same frame size.....	(17)
3. Experimental parameters for sand-box experiments.....	(23)

## CHAPTER 1 - INTRODUCTION

Just as oil and gas are trapped by large geological structures, non-aqueous phase liquids (NAPLs) can be trapped by small structures at sand/shale interfaces. Many groundwater problems in the United States involve NAPL contamination (Feenstra and Coburn, 1986; Mercer and Cohen, 1990; Cohen and Mercer, 1993). Light non-aqueous phase liquids (LNAPLs) such as gasoline or jet fuel may collect in topographic highs at sand/shale interfaces, especially if they are released below the water table or if the water table fluctuates (Whitworth, 1994; Vroblesky et al., 1995).

When NAPLs are immobilized by trapping at sand/shale interfaces they may become a long-term source of contamination because conventional pump and treat remediation methods may not adequately remove them. At the same time, NAPLs immobilized at sand/shale interfaces can only have a limited effect on the aquifer because dispersion and dilution processes will act over some finite distance to decrease dissolved NAPL concentrations below regulatory limits. Thus it is important to investigate the role of sand/shale interfaces in NAPL trapping. The purpose of this study is to investigate the potential role of small-scale DNAPL/LNAPL trapping structures at sand/shale interfaces and to determine the smallest scales(s) at which NAPL trapping may occur. A complete investigation of this topic is not within the scope of this thesis. However, guidelines based upon sand-box visualization experiments, field measurements, and calculations with Hobson's Formula are presented to provide a starting point for evaluation of trapping of spilled NAPLs at sand/shale interfaces.

Common LNAPLs include gasoline, jet, and diesel fuel. DNAPLs are commonly



chlorinated hydrocarbons and include trichloroethylene and pentachlorophenol.

Saturated zone NAPL flow is dependent upon the densities, viscosities, and interfacial tensions of the liquids as well as grain and pore size of the aquifer matrix. NAPLs are also subject to dispersion, diffusion, adsorption, and microbiological degradation (Fetter, 1993). In short, the behavior of NAPLs in the subsurface is complex. Pinder and Abriola (1986) needed 27 independent equations to develop a comprehensive model for NAPL flow.

Aquifers are naturally water wet because they contain water before any spilled NAPL enters the aquifer (Fetter, 1993). When water, or any other liquid, is in contact with a surface there is a difference between the attraction of liquid molecules for one another and the attraction between the surface and the molecules of the liquid. This difference in attraction is called interfacial tension. It is defined as the amount of work necessary to separate one unit area of the liquid from the surface. Liquid-to-liquid boundaries, such as that between water and immiscible liquids also possess interfacial tension (Fetter, 1993).

If two immiscible liquids are in contact, a curved surface develops at the interface. When the pore pressure inside each liquid is measured, it is found that the pore pressures are not the same (Fetter, 1993). This difference in pressure is the capillary pressure. Capillary pressure also develops between the water and the aquifer matrix. Capillary pressure is directly proportional to interfacial tension and inversely proportional to the radius of curvature at the contact between the two liquids. This suggests that capillary pressure is a function of not only the properties of the two immiscible liquids present, but also of the amount of each liquid present (Fetter, 1993). Capillary pressure is

also a function of the pore and pore throat geometry. For these reasons, exact capillary pressure distributions in porous media vary and are difficult to calculate. They can be determined in the laboratory for specific conditions (Fetter, 1993).

Water is attracted to mineral surfaces by interfacial tension. Therefore, some of this water is stuck rather tightly to the grains; making them water wet. This tightly bound water does not flow through the pores and is called irreducible water. The irreducible water saturation is the water content at which no additional water will flow (Fetter, 1993).

When a NAPL encounters saturated (water-wet) porous media, it must overcome the capillary pressure between the water and the NAPL in order to enter the pores. This capillary or saturation pressure is related not only to the size of the pore throats that the NAPL must pass through, but also the physical properties of the compound. The capillary pressure required for NAPL to enter very small pores can be quite high, often on the order of tens of atmospheres while the capillary pressure required for NAPL to move through the pores of coarse-grained material can be just tenths of atmospheres or less (Dahlberg, 1995). Thus NAPL can move relatively freely through sands but will not freely enter shale and can be trapped at sand/shale interfaces when sufficient closure (height of confining structure at the sand/shale interface) exists.

Capillary pressure due to grain size changes can be important even in the body of the aquifer, resulting in pore-scale capillary trapping or residual saturation (Fetter, 1993). Residual saturation is defined as the fraction of the pore space filled with immobile NAPL. However, pore-scale (residual) trapping of NAPLs is not the topic of this study.

Most NAPL spills occur at the surface, or from underground storage tanks. In the vadose zone, both LNAPLs and DNAPLs tend to follow the paths of greatest

permeability (Fetter, 1993) and tend to collect on top of finer-grained materials. When closure exists on top of these finer-grained materials, NAPLs can become trapped or pooled within the vadose zone.

Once in the saturated zone, LNAPLs tend to float on the water table while DNAPLs sink toward the base of the aquifer. Even though LNAPLs float, they can still migrate into shallow confined aquifers. Whitworth (1994) presented the following pathways for LNAPL to reach shallow confined aquifers:

- If construction, such as tank installation, breaches an overlying clay or shale layer.
- Through cracks or fractures in the clay or shale.
- Through biological structures such as root traces, etc. Palmer (1992) states these may be open to tens or hundreds of feet.
- Through earthquake-produced sand blows. During an earthquake, liquefied sand bursts through the overlying clay layer and, in many cases, leaves a fully penetrating sand-filled conduit through the overlying clay layer.

Whitworth (1994) and Vroblesky et al. (1995) also pointed out that LNAPLs could be trapped due to fluctuating water tables.

Due to their greater density, DNAPLs, depending upon spill volume, can easily migrate to significant depths. Large DNAPL releases do occur. For example, sites at Love Canal and Hyde Park each contained many thousands of tons of buried DNAPLs including chlorinated benzenes, chlorotoluenes, carbon tetrachloride, tetrachloroethene, and trichloroethene (Cohen and Mercer, 1993).

## CHAPTER 2 – FIELD WORK

### Site Geology

Sites 1 and 2 are located stratigraphically below the gradational contact between the Abo and the Yeso formations. The Permian Abo formation is typically dark red and has a continental origin as suggested by its color, and the presence of mud cracks, current ripple marks, cross-bedding, land vertebrate tracks, plant impressions and the lenticular nature of the sandstone bodies (Titus, 1963).

In the vicinity of Sites 1 and 2, the uppermost Yeso consists of thinly intercalated beds of white, fine-grained sandstones and calcareous black to dark gray and red shales. Numerous salt casts are present on the surface of the gray shales at the base of some of the sandstones. Mack and Suguio (1991) suggest that many of the Yeso shales may be playa lake facies and many of the Yeso sandstones of aeolian origin. However, they also suggest that the gray shales may be deposited in a nearshore mixed aeolian-tidal-flat environment.

Site 1 is located at latitude 34° 09' 81" N, longitude 106° 45' 00", where the Yeso sequence consists of a series of interbedded light gray, thin sandstones and slightly thicker dark to light gray and red shales (Figure 1). The sandstones range from 4 to 8 cm in thickness, are very fine-grained, well-cemented, and consist mostly of subrounded quartz grains and are probably aeolian in origin. The gray shales are hard and fissile and locally contain thin fracture infillings of azurite and malachite and range from 46 to 61 cm in thickness in the vicinity of Site 1. The red shales are typically silty and sometimes sandy and are typically of similar thickness to the gray shales in the vicinity of Site 1.

The upper sandstone surface that was examined at Site 1 has a strike of S 70° W and

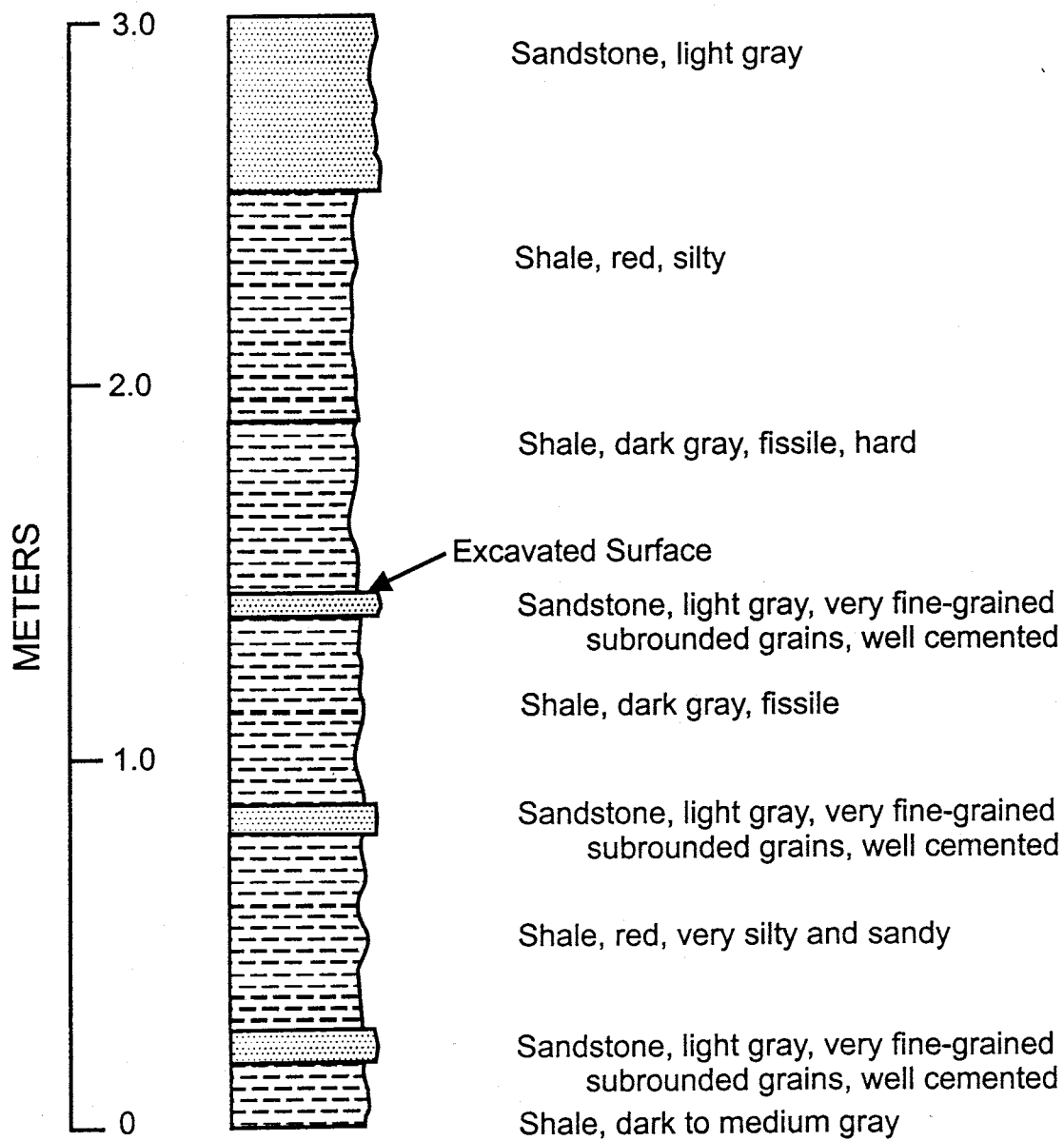


Figure 1. Measured section from Site 1 showing location of excavated surface. This site is located in Permian, upper Yeso Formation rocks.

generally dips  $8^{\circ}$  N  $20^{\circ}$  W. The surface relief on this sandstone body consists of small, cm-scale hummocky topography and a few more widely spaced (tens of cm to meters) 1 to 1.5 cm deep load casts (Figure 2). The surface is also fractured. The fractures are in two regularly-spaced sets that trend N  $31^{\circ}$  W and N  $62^{\circ}$ W. The fractures are more prominent on the weathered surface of the sandstone than they are on the excavated surface where they tend to be only one or two mm in width. There are no obvious faults within 100 m of Site 1, although there are several large normal faults with throws greater than 30 m within 500 m of the site.

Site 2 is located at latitude  $34^{\circ} 09' 84''$  N, longitude  $106^{\circ} 45' 00''$  and is approximately 15 m stratigraphically lower than Site 1. Here the Yeso consists of a sequence of intercalated red silty shales and red silty sandstones (Figure 3). The shales in the vicinity of this site range from 43 to about 90 cm in thickness and the sandstones range from 30 to 91 cm in thickness. The sandstone surface we examined has a strike of S  $75^{\circ}$  W and dips between  $10$  and  $16.5^{\circ}$  in a generally N  $15^{\circ}$  E direction. This change in dip may be the result of minor folding associated with normal faulting. A vertical fault with in excess of 18 m of throw is located approximately 37 m E of Site 2. The surface of the sandstone exhibits a cm-scale hummocky topography (Figure 4). No obvious load casts were observed. The sandstone is also fractured and the fracture sets trend N  $15^{\circ}$  E and N  $89^{\circ}$  E, although the fractures sets at this location are less regularly distributed than at site 1. Again, the excavated surface is less fractured than the weathered surface although the fracture frequency of the excavated surface at Site 2 is less than at Site 1. Site 3 is located in the Miocene Popotosa Formation at latitude  $34^{\circ} 13' 50''$  N,

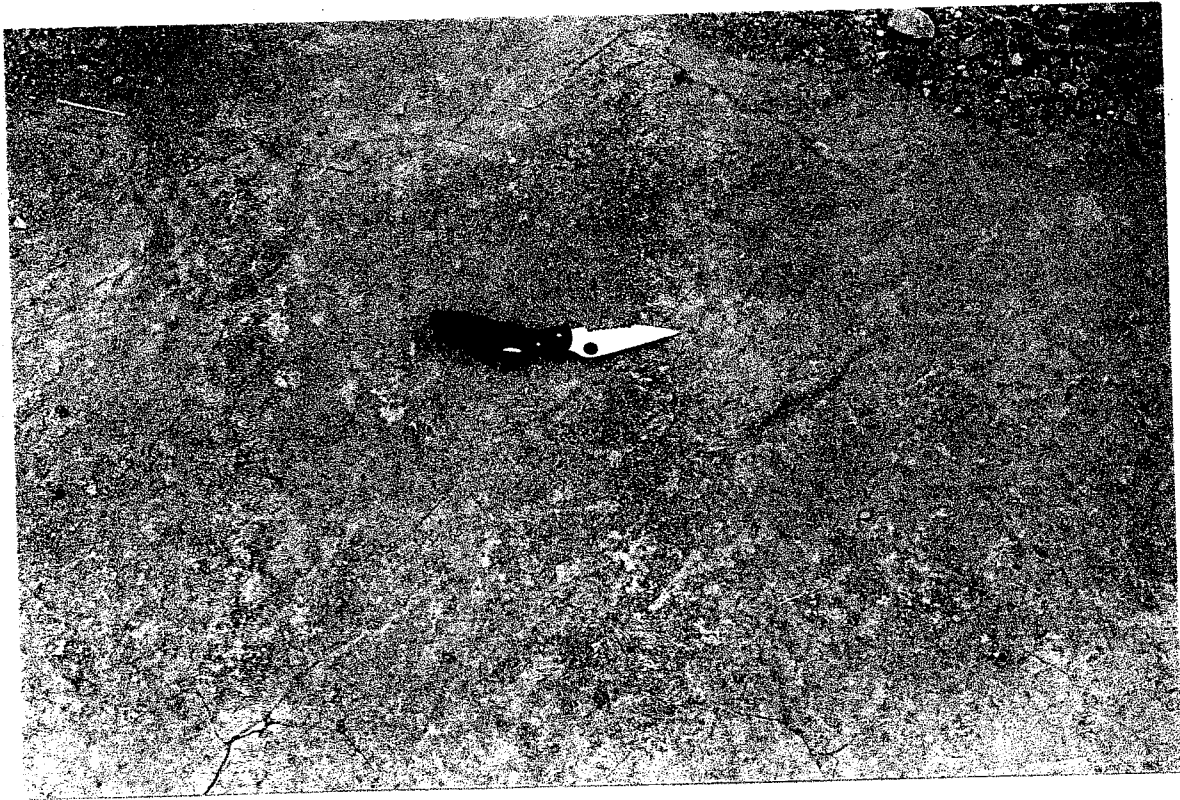


Figure 2. Photograph of the excavated sandstone surface at Site 1. The knife in the photograph is 22 cm in length. The surface exhibits hummocky, cm-scale topography, scattered small cm-scale load casts, and fractures.

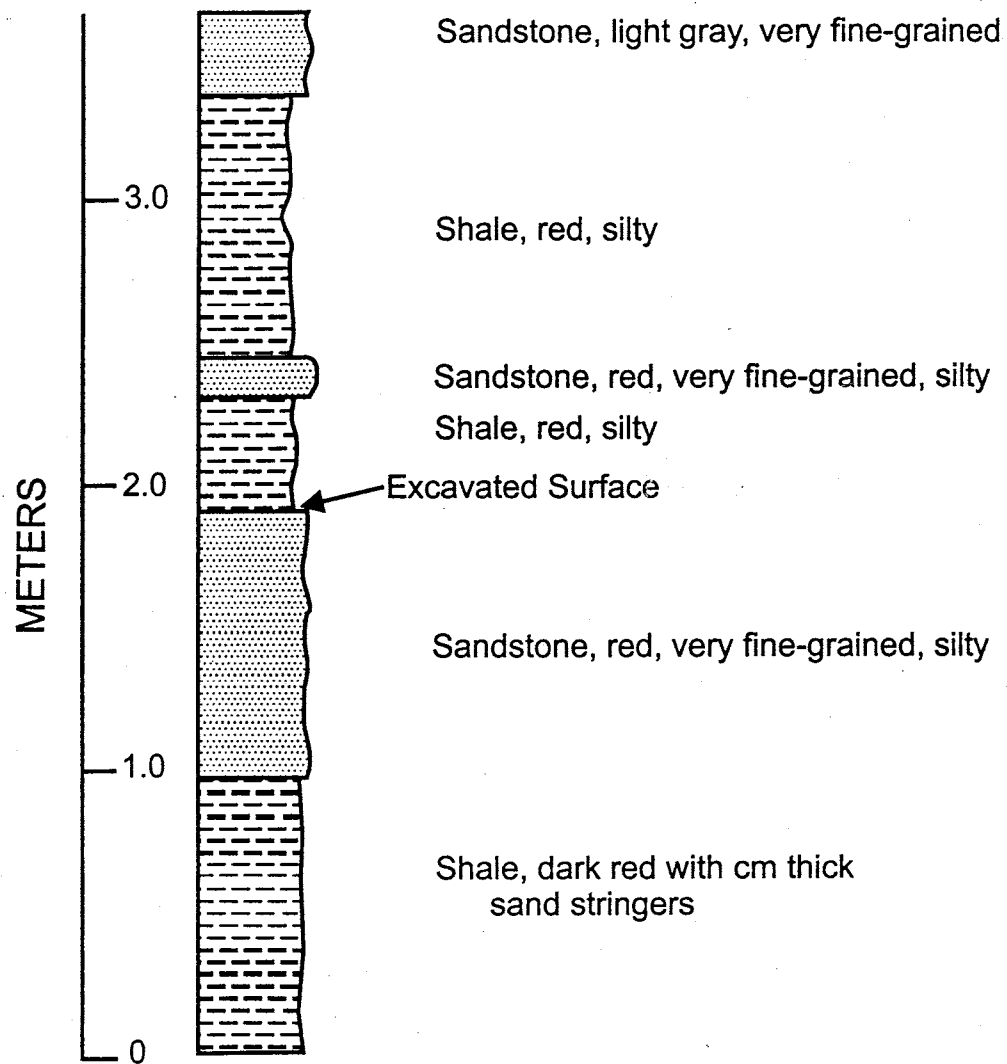


Figure 3. Measured section from Site 2 showing location of excavated surface. This site is located in Permian, upper Yeso Formation rocks.





Figure 4. Photograph of the excavated sandstone surface at Site 2. The knife in the photograph is 22 cm in length. This surface is more heavily fractured than that at Site 1 and exhibits a similar cm-scale hummocky topography. There are no identifiable load casts at this site.

longitude 106° 59' 06". The Popotosa formation was deposited in a broad, closed sedimentary basin which developed due to crustal extension associated with formation of the Rio Grande Rift (Meyer, 1983). This basin was filled by coalescing alluvial fans along the surrounding uplifted areas and graded into playa lakes on the basin floor (Chamberlin, 1980, 1981). The stratigraphy at Site 3 consists of intercalated distal alluvial fan sands and playa muds or shales (Figure 5). The sandstones range in thickness from 11 cm to 22 cm and the shales range in thickness from 9 cm to 54 cm at this site. The sandstones are a dark reddish brown in color and exhibit a coarsening upward sequence in which the lower portion of the beds is uniformly fine-grained but the uppermost few cm contains a significant portion of coarse grains. The sandstones are commonly well-cemented. The shales are light gray, soft, and crumbly.

The topography on the excavated portion of the upper sandstone surfaces (Figure 6) is due to a combination of penecontemporaneous deformation due to uneven loading and small-scale tectonic stress. The surface exhibits a cm-scale hummocky topography with a general N 20° E trend for the longer features. There are no obvious load casts on the surface, although there are some shale clasts (1.5 – 6 cm diameter) present in the top of the sandstone. The white spots in Figure 3 are remnants of plaster from plaster casts taken on this surface.

The sandstone surface is fractured and the fracture sets trend N 45° E and N 9° E. The fractures are significantly less prominent on the excavated surface than on the exposed, weathered surfaces in the vicinity. There is a small fault located about 2 m northwest of the excavated surface at Site 3. This normal fault has a throw of 28 cm. Another small normal fault with an apparent throw of several meters lies 20 m north of

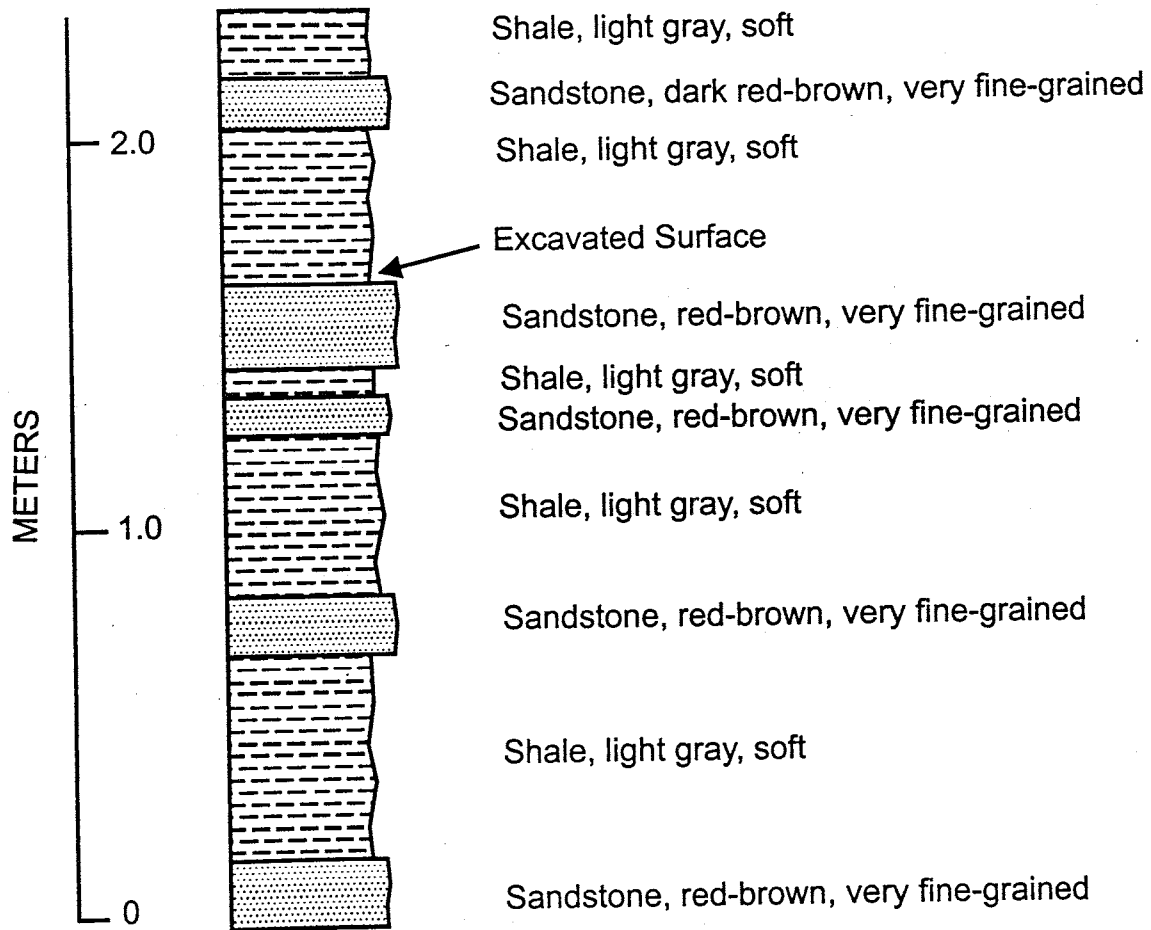


Figure 5. Measured section from Site 3 showing location of excavated surface. This site is located in the Miocene Popotosa Formation.



Figure 6. Photograph of the excavated upper sandstone surface at Site 3. The knife in the photograph is 22 cm in length. Topographic variation on this surface seems to be the result of penecontemporaneous deformation due to loading as well as due to tectonic stress from faulting and erosion. The fractures are thought to be caused by stress from erosion and faulting.

the excavated surface. Some gentle folding is apparent in the vicinity of site 3 because the dip angles on the sandstone beds range from a low of  $1^{\circ}$  to a high of about  $15^{\circ}$  over an area of about 100 square meters.

## **Methods**

I carefully excavated a number of sand/shale interfaces for study. All study sites were in Socorro County, New Mexico. Further information on the locations and geological descriptions of these sites is given in Appendix A. After considerable effort expended toward constructing digital elevation models of the surfaces, from which I attempted to map closure, I found that it was simpler to pour plaster molds of the surfaces. Sixty-two square wooden frames were built and sealed to the excavated outcrops with natural clay caulking, and then filled with plaster. I measured the data on these plaster molds.

I measured the closure volume of each plaster cast in the laboratory using a mass balance technique. The plaster casts were first sealed with varnish because plaster tends to absorb water. Then each plaster cast was placed on a large plaster funnel frame. This funnel frame was designed to funnel water poured over the plaster cast into a pre-weighed beaker. The mass balance measuring procedure is as follows:

1. Place the plaster cast on the funnel frame.
2. Pour deionized waters into a pre-weighed beaker and record the weight of water.
3. Pour water over the plaster cast until it fills all of the low spots and runs over onto the funnel frame and into another pre-weighed beaker.
4. Weigh the water remaining in the beaker.

5. Carefully dab up all remaining drops of water on the sides of the plaster cast frame and the funnel with pre-weighed lab-wipes and record the damp weight.
6. Calculate the volume of water remaining in the low spots from

$$W_t = W_i - (W_c + W_{cw}) \quad (1)$$

Where  $W_t$  is the weight of water trapped (g),  $W_i$  is the initial weight of water used (g),  $W_c$  is the weight of water collected (g), and  $W_{cw}$  is the weight of water absorbed by the Chemwipes™. Since the density of water is very close to 1.0 g/cm<sup>3</sup>, Equation 1 can be used to calculate the volume of water trapped.

All of the plaster casts were taken on the excavated surface of sandstones immediately below the overlying shales. Therefore, when the plaster casts were inverted for measurement, the hollows represented potential LNAPL traps because on the actual sand surface they represent inverted bowl-shaped structures. The lower sand surfaces were not quantitatively investigated, but visual examination suggests that topographic variation on these surfaces is similar to that on the upper surfaces.

Four mass balance measurements were performed on each plaster cast. The results of the first measurement were discarded because there was some water absorption during this first wetting. The mass balance measurement single standard deviation precision for the following three measurements averaged  $\pm 1.4$  percent.

The topographic variability of the surface is also an important parameter. Therefore, a frame was constructed that fit over the plaster casts and used as a reference to measure the height of the surface at 36 points for each plaster cast. This data was then normalized to the lowest elevation reading on each plaster cast so that the reported

numbers can be interpreted as actual topographic variation. Height measurements were taken with a digital depth gage accurate to 0.01 mm.

## Results

Closure volume measured from the plaster casts ranged from a low  $0.56 \text{ L/m}^2$  to a high of  $2.88 \text{ L/m}^2$  for the sand/shale interfaces examined. The average for all 62 locations at the three sites was  $1.22 \text{ L/m}^2$ . For an assumed average porosity of 30 percent, this translates to maximum potential trapping capacities ranging from  $0.17$  to  $0.86 \text{ L/m}^2$  with an average of  $0.37 \text{ L/m}^2$ .

Three different sized frames were used at site 1 to see if the measured closure volumes exhibited a scaling trend (see Table 1 & Table 2). There was no general increase of closure volume with frame size. Therefore, the frame size of  $1024 \text{ cm}^2$  provides reasonably accurate results. The mean closure volume at Site 1 ( $n = 41$ ) was  $1.11$  with a standard deviation of  $0.25 \text{ L/m}^2$ . The maximum was  $1.65$  and the low was  $0.68 \text{ L/m}^2$ . The mean closure at Site 2 ( $n = 12$ ) was  $1.17$  with a standard deviation of  $0.19 \text{ L/m}^2$ . The maximum was  $1.48$  and the minimum was  $0.89 \text{ L/m}^2$ . At Site 3 ( $n = 9$ ), the mean was  $1.43$  with a standard deviation of  $0.79 \text{ L/m}^2$ . The maximum was  $2.87$  and the minimum was  $0.56 \text{ L/m}^2$ . The closure volumes reported here should be interpreted as minimum values due to possible edge effects. The statistical distribution relationship between the closure volumes and frame sizes are listed in Table 2.

Table 1. Site 1 summary data.

No. of measurements	Mean closure volume (L/m <sup>2</sup> )	Frame size (cm <sup>2</sup> )	Maximum (L/m <sup>2</sup> )	Minimum (L/m <sup>2</sup> )	Std. Dev. (L/m <sup>2</sup> )
21	1.12	1024.00	1.65	0.68	0.25
10	1.20	1451.61	1.55	0.91	0.20
10	1.15	2090.32	1.48	0.98	0.15

Table 2. Summary data for different sites with same frame size

Location	No. of measurements	Mean closure volume (L/m <sup>2</sup> )	Frame size (cm <sup>2</sup> )	Maximum closure volume (L/m <sup>2</sup> )	Minimum closure volume (L/m <sup>2</sup> )
Site 1	21	1.12	1024.00	1.65	0.68
Site 2	12	1.17	1024.00	1.48	0.89
Site 3	9	1.43	1024.00	2.87	0.56

The actual closure height for individual traps were difficult to measure. However, the maximum closure height at an interface cannot be greater than the maximum relief at that interface. Therefore, topographic variation was used as an indicator of maximum closure height.

At site 1, the maximum topographic variation was 2.4 cm, and the mean was 1.3 cm. At site 2, the maximum was 3.3 cm and the mean was 2.0 cm. At site 3, the maximum was 4.8 cm and the mean was 2.4 cm. Greater topographic variation exists at larger scales on sand/shale interfaces, especially in intermontane valleys (Love et al., 1997). However, larger scales were not examined in this study.



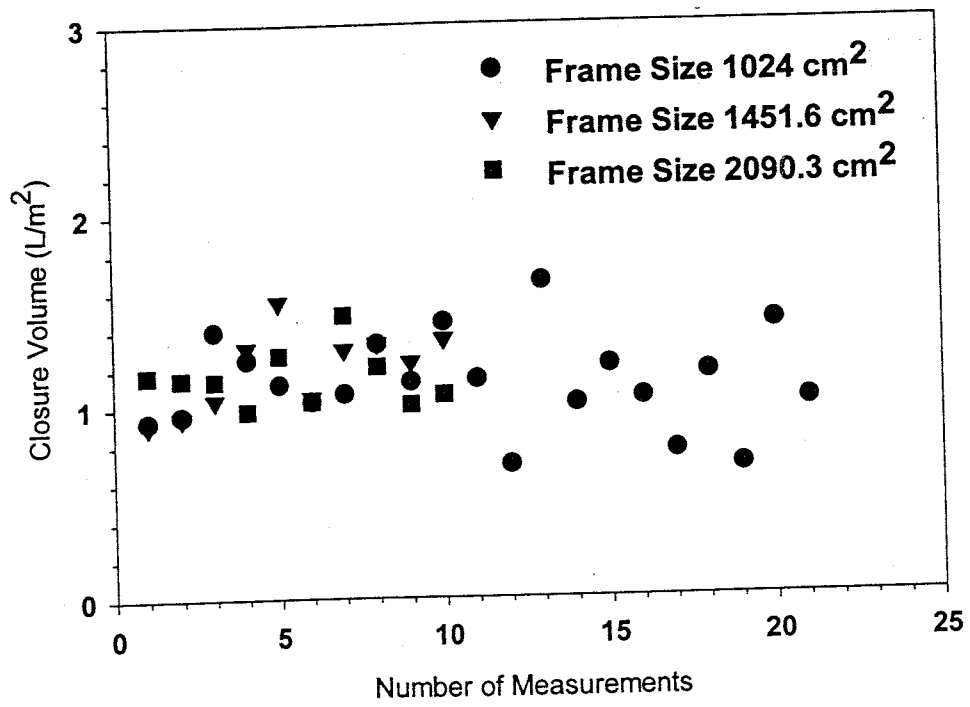


Figure 7. Closure volume versus frame size for site 1.

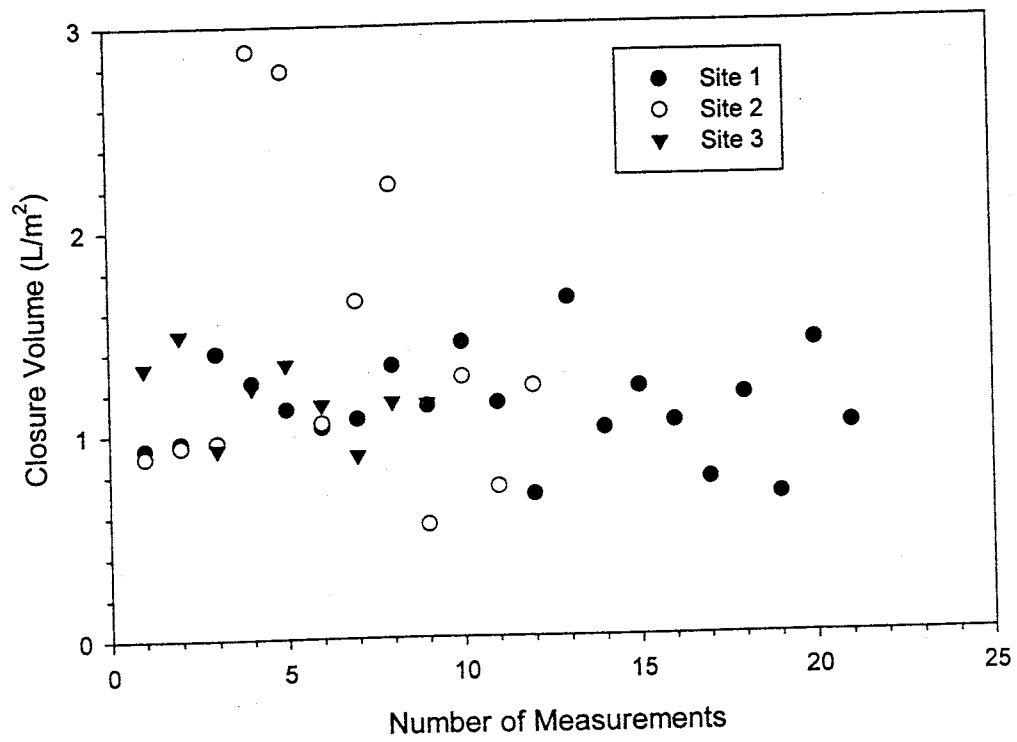


Figure 8. Closure volume for frame size 1024 cm<sup>2</sup> for all sites.

## CHAPTER 3 - SAND BOX EXPERIMENTS

### Previous Work

Most of the research concerning the movement of NAPLs in the subsurface has been conducted in the fields of petroleum and soil science. Van Geel and Sykes (1994) conducted a NAPL spill saturation distribution simulation in the laboratory by using image analysis technologies. Zalidis et al., (1991) developed an experimental technology by using a soil column apparatus to monitor the movement under unsaturated flow conditions of dissolved volatile compounds from an immobile NAPL source. Their experiments try to expand the study of the long and short-term behavior of immobile volatile multi-component NAPL's in soil contamination. By using different sand sizes and NAPL compounds, Schroth et al, (1995) developed two-dimensional experiments in a glass chamber visualization experiment to delineate the changing LNAPL lens boundary during the infiltration process. This study examines the potential role of trapping features at sand/shale interfaces in immobilizing spilled NAPLs.

### Material, Apparatus, and Procedure

A sand-box was constructed from a solid piece of 1.90 cm thick aluminum plate. The opening was milled out and included a 4 by 8 cm trap along the upper surface of the cutout. O-rings were set 0.16 cm from the edge of the opening (Figure 9). A fluid input port, a fluid output port, and a fill port in the top of the trap were drilled and tapped 1/8" NPT.

The sand-box was assembled by clamping 0.64 cm thick glass plates to the sides of the sand box with small c-clamps. The o-rings provide the seal between the glass

plates and the aluminum sand-box frame. Fine screens were placed into the inlet and outlet ports to keep the glass beads from piping out of the sand-box during the experiments, and the tubing fittings were then screwed into place in these outlets. The sand-box was then filled by pouring the proper size glass beads into the fill port with periodic firm shaking to settle and compact the beads. Next a 1/8" NPT plug was lightly screwed into the fill port. A Masterflex™ tubing pump was then connected to the inlet port and the outlet port was connected to a waste container. The sand-box was then slowly saturated with water. The plug in the top fill port was tightly screwed into place as soon as water began flowing out of the top port. Otherwise air bubbles would accumulate in the trap and it would be difficult to saturate this portion of the sand-box. Marvel Mystery Oil™ was chosen as the LNAPL because it is readily available, is relatively nontoxic, and has bright red color which gives a good visual contrast. After the sand-box was saturated with water, Marvel Mystery Oil™ was valved through the tubing pump and the oil slowly displaced the water in the sand box. This water displacement process assured that the beads would be water-wet as are most of the sediments at NAPL contaminated sites. Next, water was again pumped through the oil-saturated sand-box, much like would occur as a natural NAPL plume migrates along a sand/shale interfaces. Photographs were taken during the process to record the results. Several experiments were run with different bead sizes.

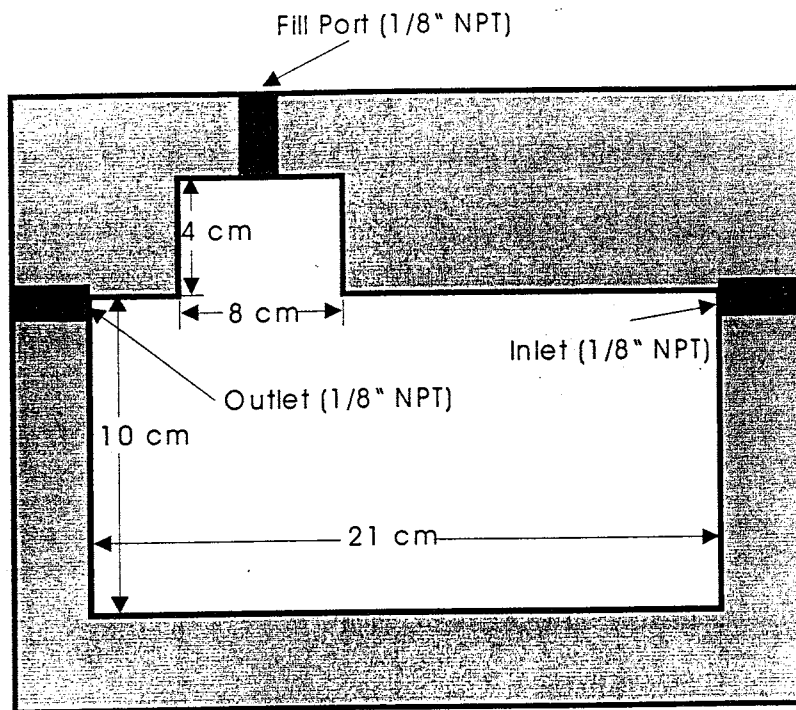


Figure 9. Schematic of sandbox used in NAPL visualization experiments

## Results

The sand box visualization experiments were designed to determine if small-scale trapping features at sand/shale interfaces can trap NAPLs. Four sand-box visualization experiments were performed. Table 3 shows the parameters for the four experiments.

Table 3. Experimental parameters for sand-box experiments

Experiment	Grain Size (mm)	NAPL	Flow rate (cm <sup>3</sup> /min)	Run time
1	1.5	Marvel Mystery Oil™	55.5	2h 20'19"
2	0.5	Marvel Mystery Oil™	40.5	1h 20'
3	0.2	Marvel Mystery Oil™	55.5	12'00"
4	0.2	Marvel Mystery Oil™	55.5	13'10"

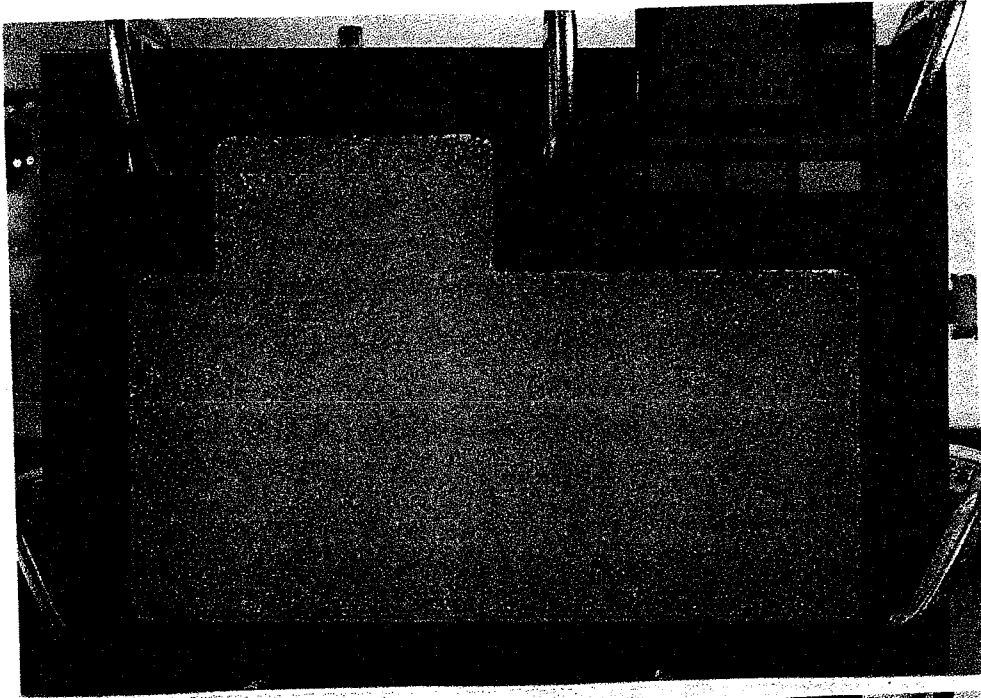
The first run used 1.5-mm diameter glass beads as a porous medium. The bead size is equivalent to very coarse sand. The sand-box was first saturated with water (Figure 10A). Next, Marvel Mystery Oil™, which has a bright red color and therefore gave good contrast in the photographs, was allowed to enter the sandbox. Notice in Figure 10B that the oil has just begun to flow into the beads through the input port on the right side of the photograph. Flow is from right to left in each photograph. Oil was pumped into the sand-box until it was essentially saturated with oil. Figure 10C shows the water in the sand-box being displaced by oil. Figure 10D shows the sand-box almost completely saturated with oil. After the oil filled the sand-box, water was again input and began to displace the oil. Figure 10E shows the sand-box after about half the oil has been displaced by water. Figure 10F shows the sand-box at the end of the experiment (2 hours and 20 minutes) where steady state had been reached and no more oil flowed from the

sand-box. Notice that the 4 by 8-cm trap is almost completely saturated with oil at this point and that the rest of the sand-box is at residual saturation. The base of the oil in the trap was slightly tilted toward the exit port due to the advective force of flowing water (for more information on this phenomenon see Fetter, 1993, or Dahlberg, 1995). The flow rate through the sand-box during this experiment was  $55.5 \text{ cm}^3/\text{min}$ .

The second run used 0.5 mm glass beads. This bead size lies on the boundary between medium and coarse sand. The procedures were identical to the first experiment. The flow rate for this experiment was  $40.5 \text{ cm}^3/\text{min}$ . Figure 11A shows the sand-box initially saturated with water and Figure 11B shows the oil beginning to displace the water. This continued (Figure 11C) until the sand-box was saturated with oil (Figure 11D). Then, water was pumped into the sand-box to displace the oil. Figure 11E shows the sand box after much of the oil had been displaced. Notice that the oil in the trap was already being displaced. By the end of the experiment at 1 hour and 20 minutes, the sand-box and the trap remained at residual saturation (Figure 11F).

Both the third and fourth experiments used 0.2 mm beads. This grain-size is equivalent to fine-grained sand. Otherwise the procedures were identical to the first two experiments except that neither the third nor the fourth experiments ran to completion. In the third experiment, the screen in the outlet port was too coarse and let too many glass beads through during the experiment resulting in noticeable settling within the sand-box. The photograph in Figure 12A was taken soon after the oil began to be displaced by water. Notice that the beads have settled significantly along the upper surface adjacent to the input port on the right side of the photograph. The settling resulted in the water flux

A



B

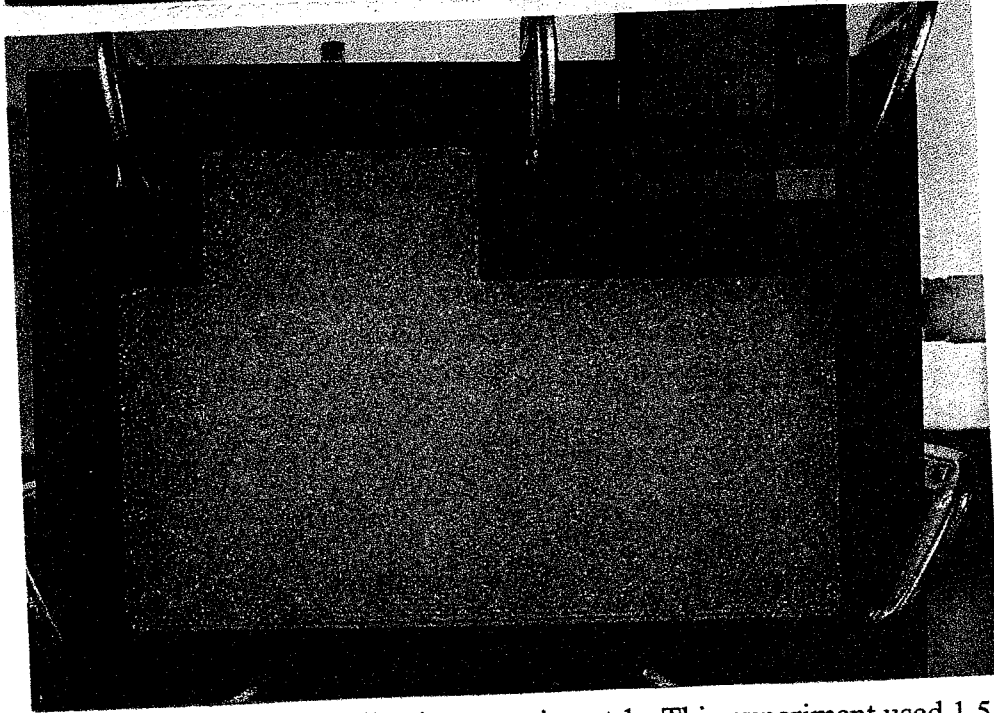


Figure 10. Results of sand box visualization experiment 1. This experiment used 1.5 mm diameter glass beads as a porous media, tap water as the wetting fluid, and Marvel Mystery Oil™ as the LNAPL. Photograph shows the sand-box after initial saturation with water. Photograph B was taken as the oil began to flow into the sand-box from left to right. Note the darker color of the oil at the middle right hand side of the photo as it enters the porous media through the inlet port.



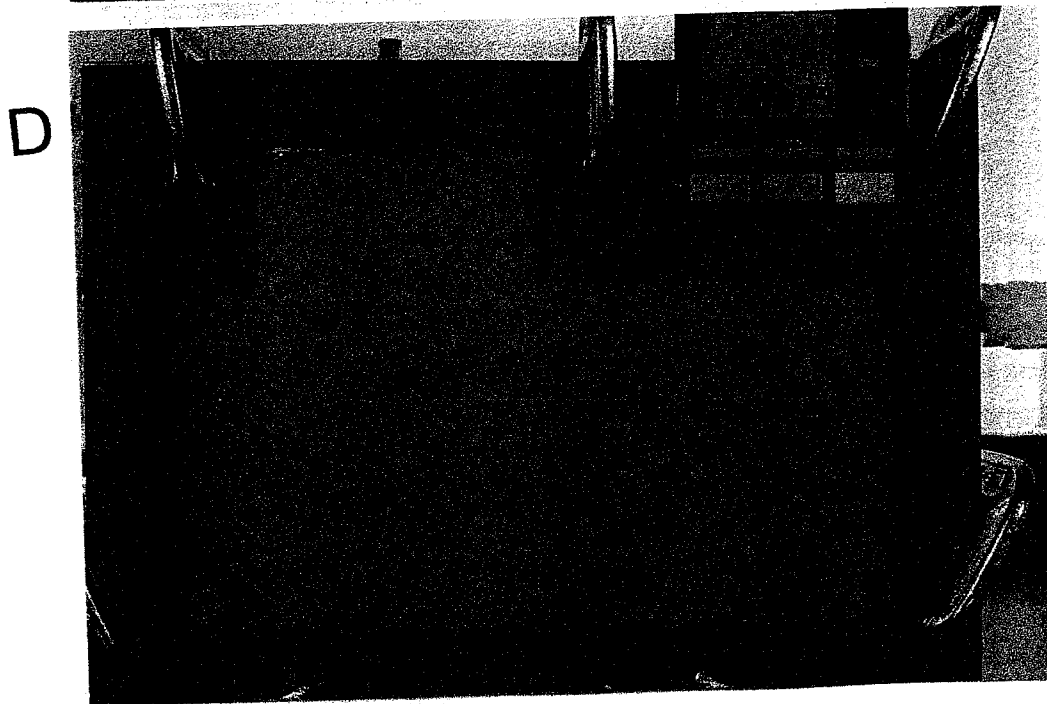
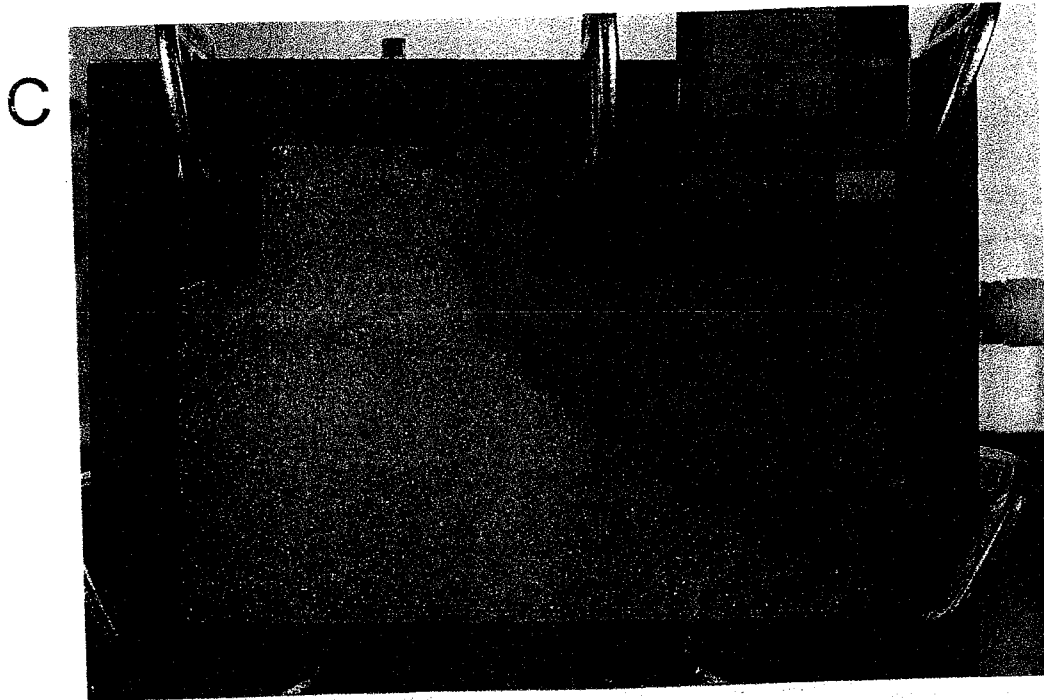
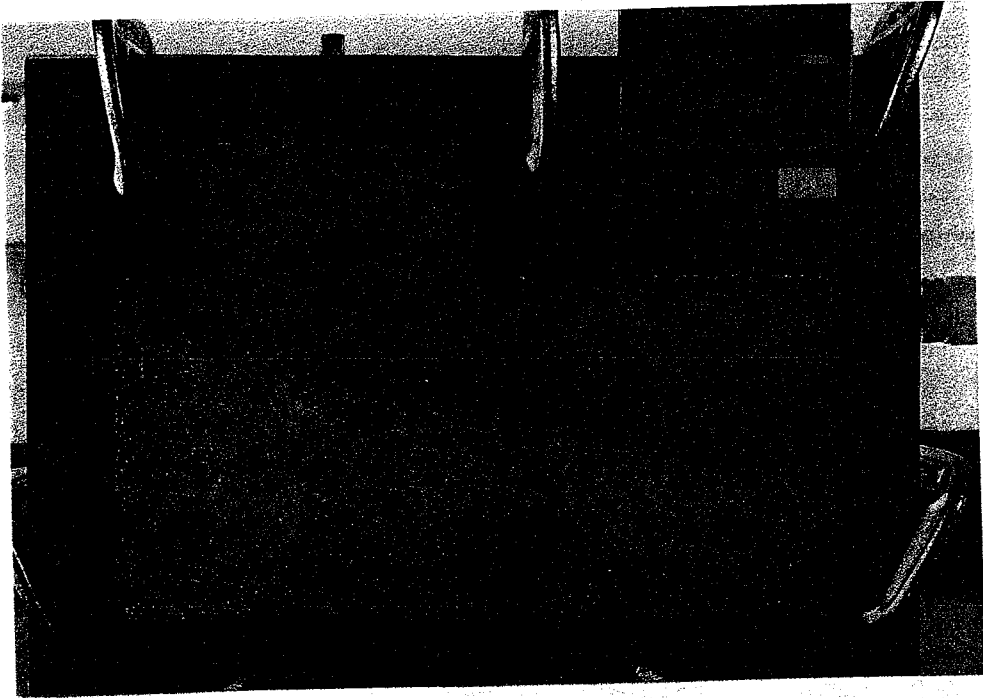


Figure 10 continued. Results of sand box visualization experiment 1. Photograph C shows the oil front invading the sand-box from right to left. Photograph D shows the sand-box almost completely saturated with oil.

E



F

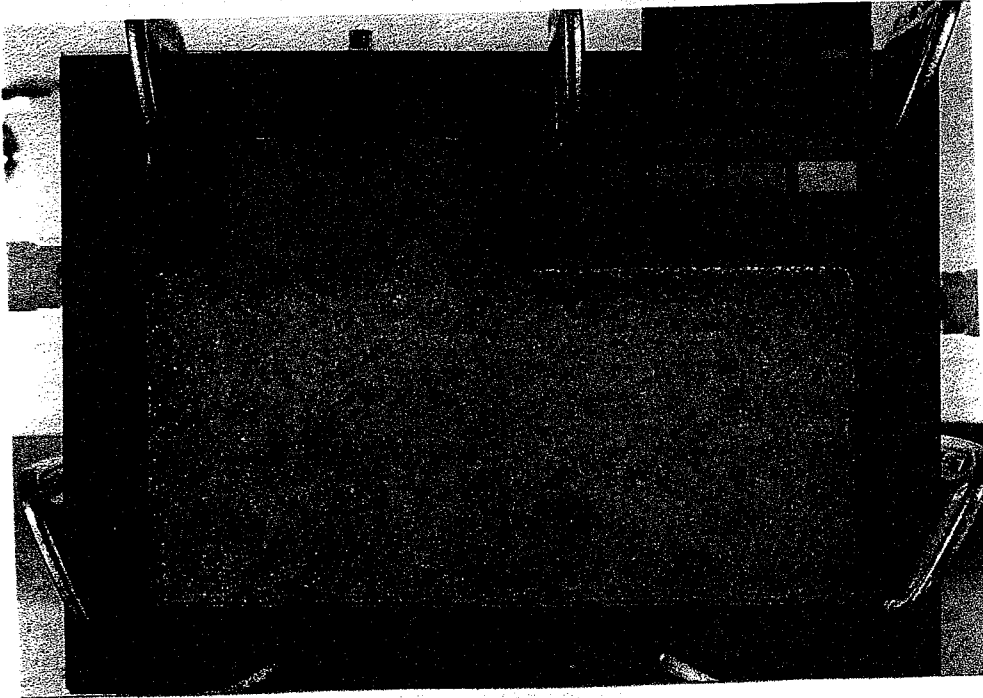


Figure 10 continued. Results of sand-box visualization experiment 1. Photograph E shows the oil being displaced by a water flood. Photograph F was taken after 2 hours and 20 minutes when oil had ceased to flow from the sand-box. Note that the trap is still full of oil at the end of the experiment.

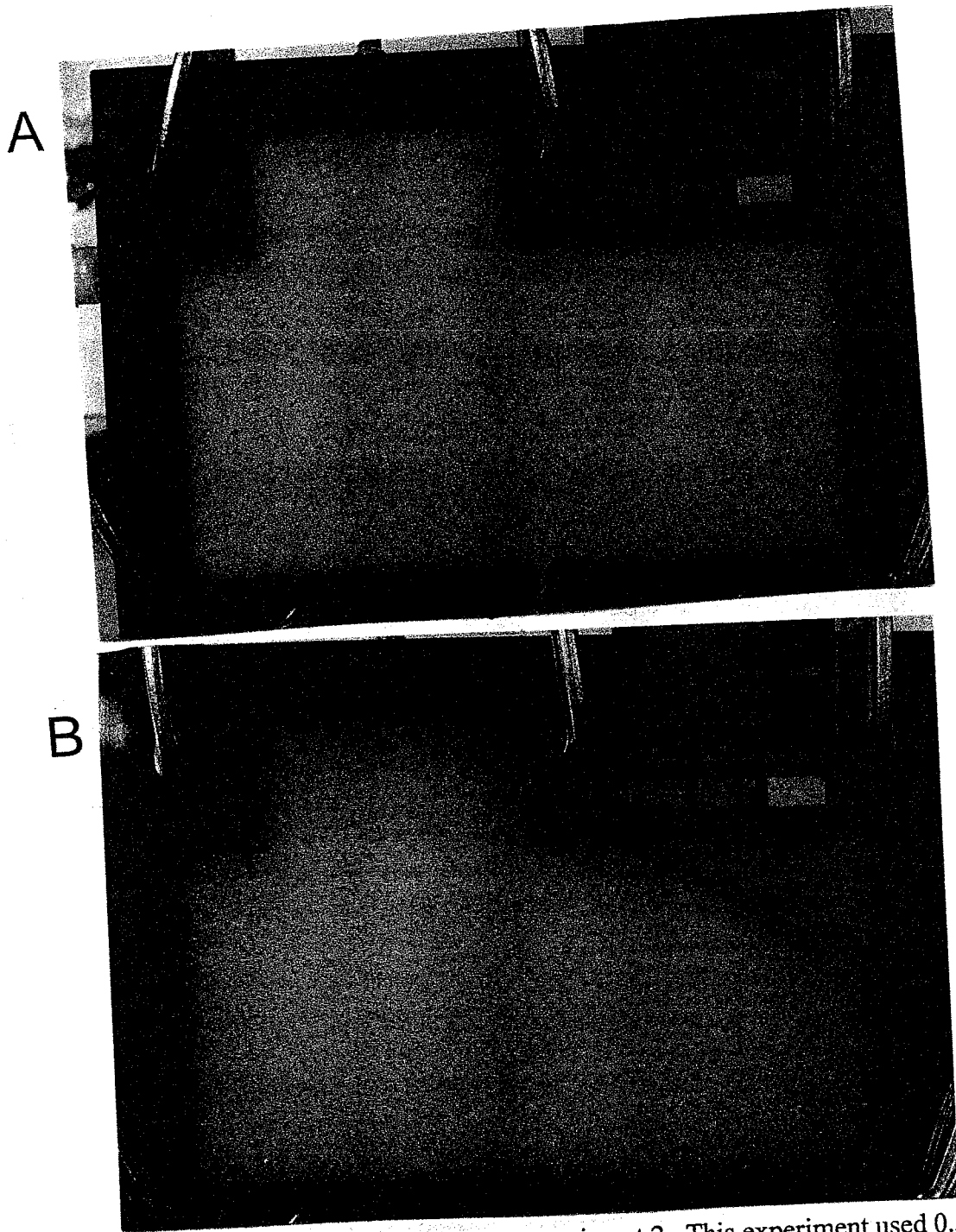


Figure 11. Results of sand-box visualization experiment 2. This experiment used 0.5 mm diameter glass beads as a porous media, tap water as the wetting fluid, and Marvel Mystery Oil™ as the LNAPL. Photograph A shows the sand-box after initial saturation with water. Photograph B was taken as the oil began to flow into the sand-box from right to left. Note the darker color of the oil at the middle right hand side of the photo as it enters the porous media through the inlet port.

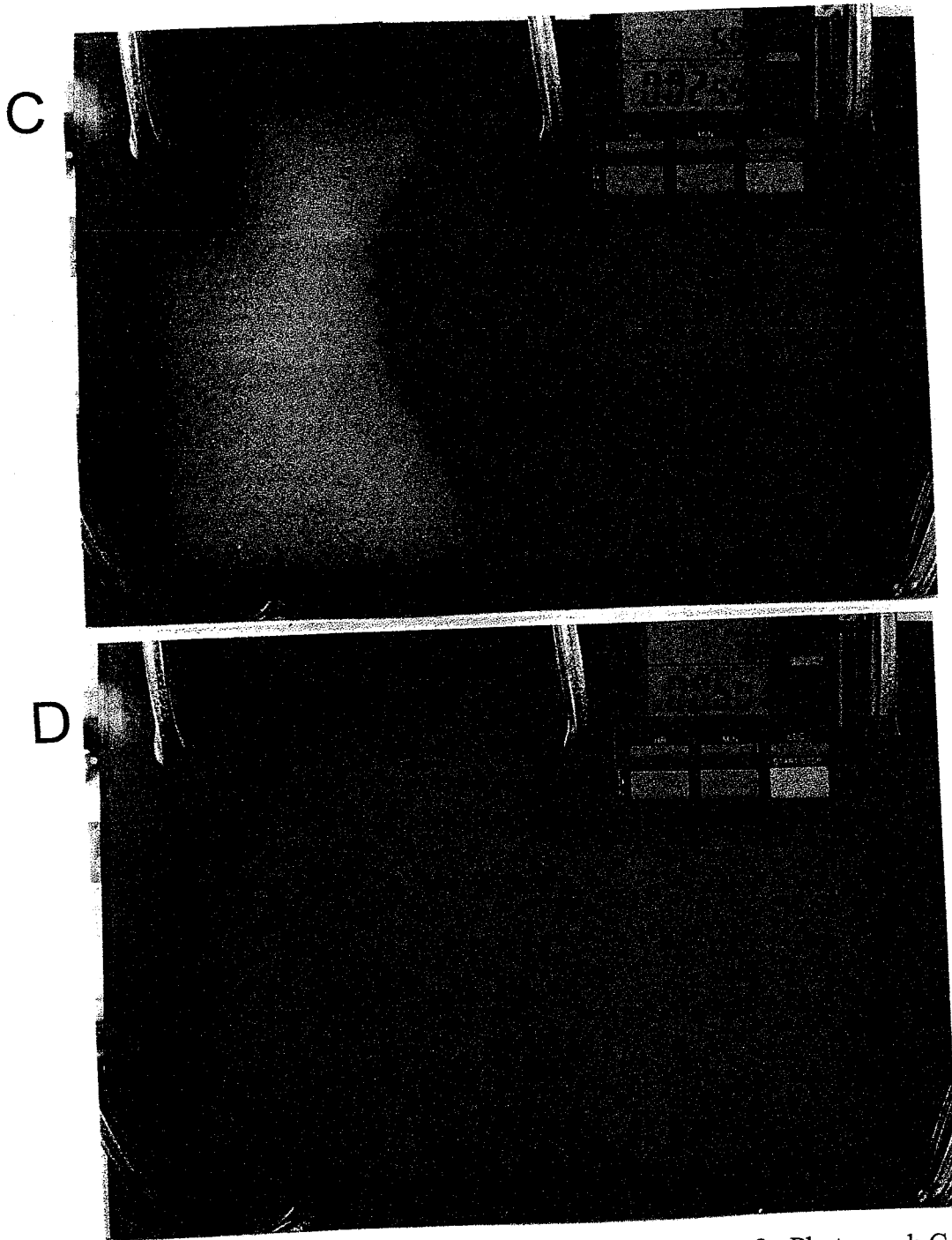
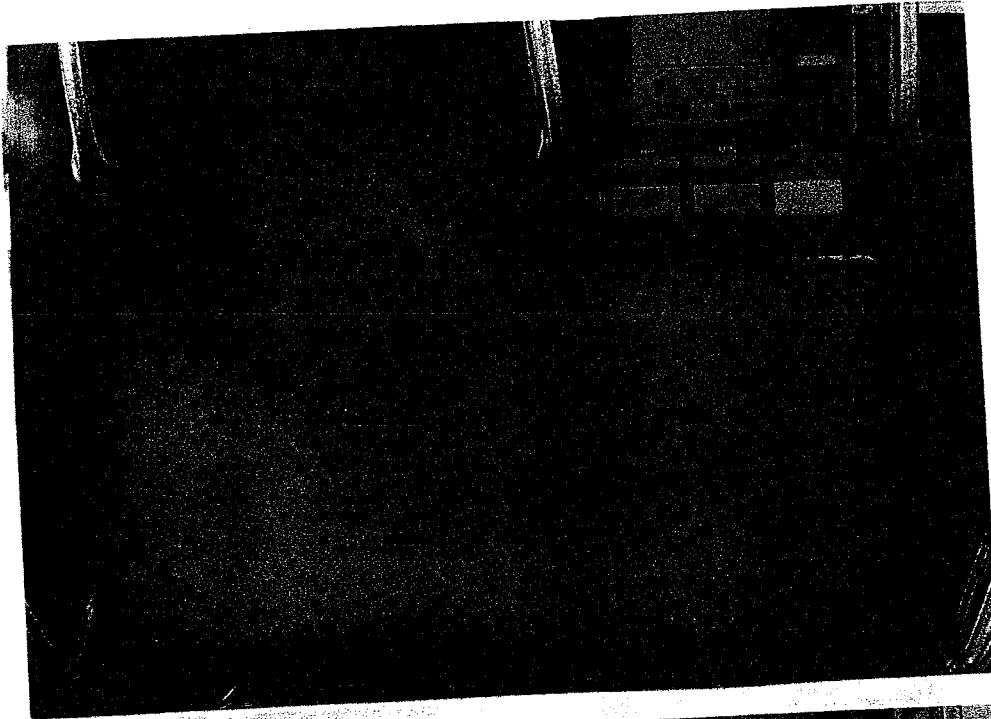


Figure 11 continued. Results of sand box visualization experiment 2. Photograph C shows the oil front invading the sand-box from right to left. Photograph D shows the sand-box almost completely saturated with oil.

E



F

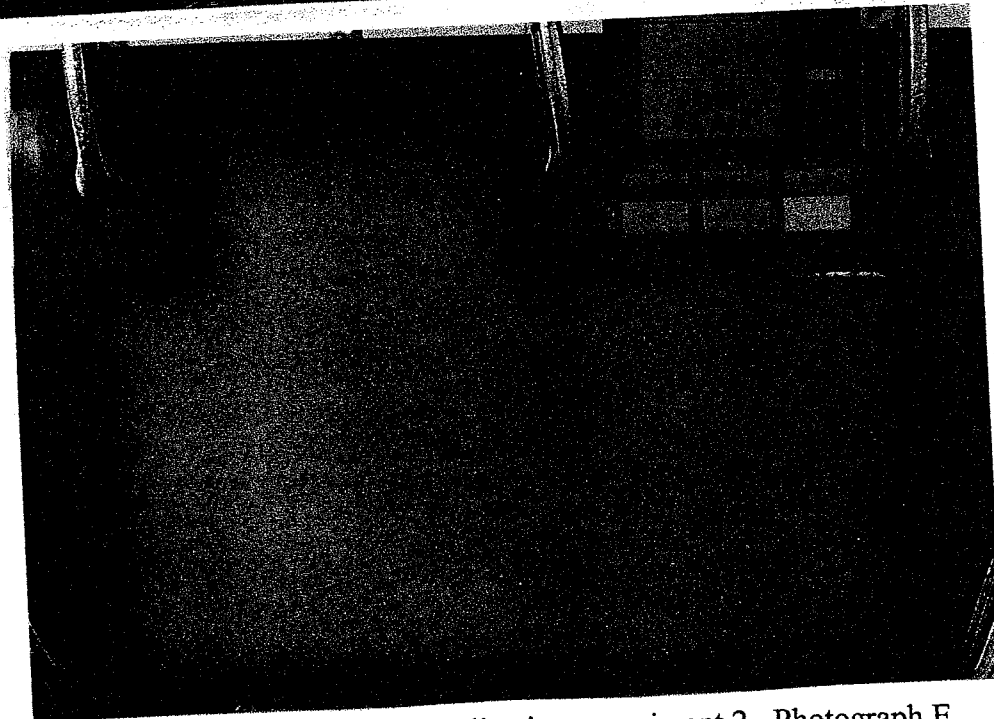
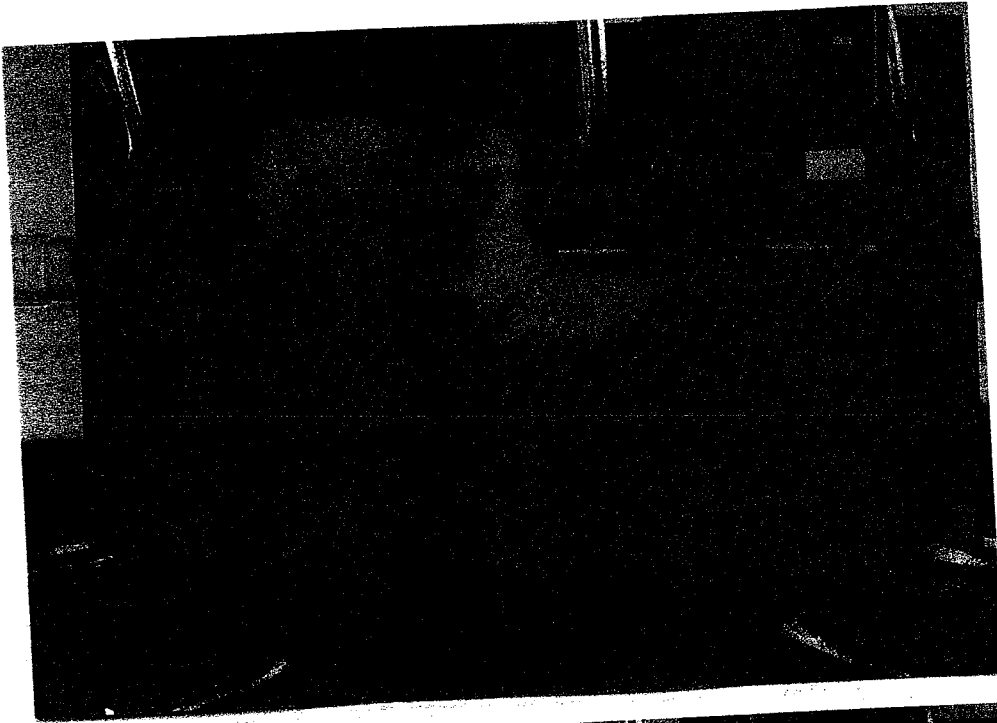


Figure 11 continued. Results of sand box visualization experiment 2. Photograph E shows the oil being displaced by a water flood from right to left. Photograph F was taken after one hour and 20 minutes. Note that the trap holds oil only at residual saturation and the pores are not saturated with oil.

A



B

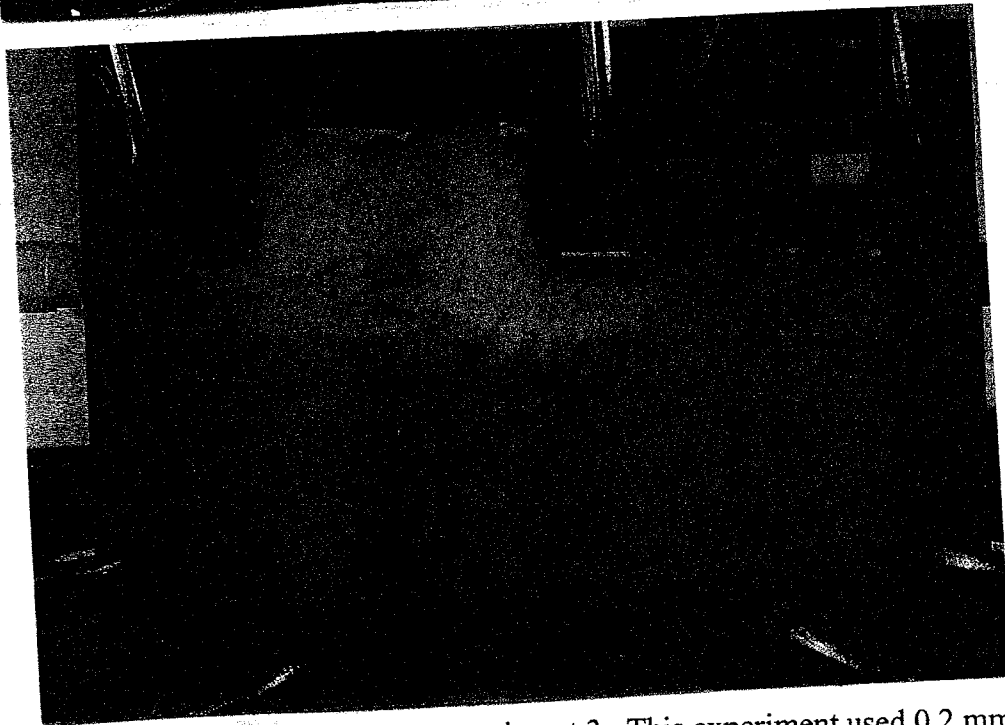


Figure 12. Results of sand box visualization experiment 3. This experiment used 0.2 mm diameter glass beads as a porous media, tap water as the wetting fluid, and Marvel Mystery Oil™ as the LNAPL. The top photograph was taken after the sand-box was saturated with oil and water flood was initiated (A). Notice that the trap is already beginning to empty. The bottom photograph was taken at only 12 minutes into the run (B), notice that the trap is already at residual saturation.

bypassing the less permeable glass beads below the settled zone. As a result, the oil was not displaced from the area below the settled zone. However, that the trap began to empty of oil quite early and by the end of the experiment it remained at residual saturation (Figure 12B). Further settling of the glass beads occurred at the top of the trap.

The fourth experiment was terminated early for two reasons. First, there was some bead loss and settling even though the screens were replaced with coarse filter paper. A perfect seal was probably not obtained with the filter paper. Second, the glass cracked before the end of the experiment. Even though this experiment did not run to completion, the results are interesting. The photograph in Figure 13A was taken after the oil began to be displaced by water. Notice that again there was some settling. Not only did the glass beads settle adjacent to the input port, but also a void developed in the upper right hand portion of the trap. This void was about  $\frac{1}{2}$  cm long and  $\frac{1}{4}$  cm high. It was beginning to fill with oil even though the grains around it were being flushed. By the end of the experiment (Figure 13B) this void was saturated with oil even though the finer-grained beads around it remained at residual saturation. The flow rate during the third experiment was  $55.5 \text{ cm}^3 / \text{min}$ . The flow rate during the fourth experiment was  $55.5 \text{ cm}^3 / \text{min}$ .

A



B

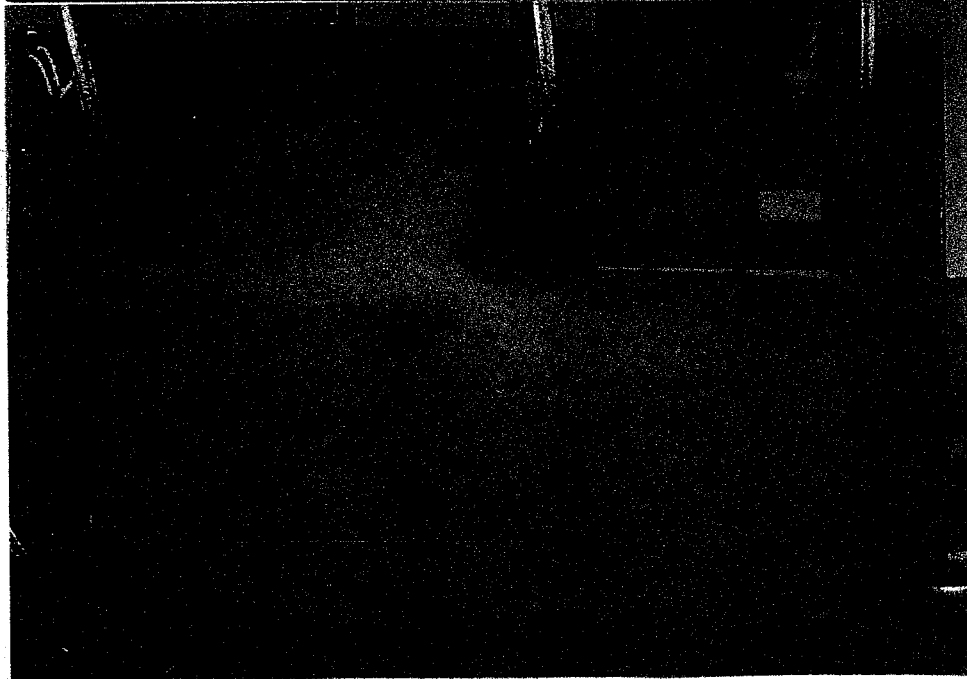


Figure 13. Results of sand-box visualization experiment 4. This experiment used 0.2 mm diameter glass beads as a porous media, tap water as the wetting fluid, and Marvel Mystery Oil™ as the LNAPL. The top photograph was taken after the sand-box was saturated with oil and water flood was initiated (A). Notice that the trap is already beginning to empty. The bottom photograph was taken at only 13 minutes into the run (B), notice that the trap is already at residual saturation. The interesting thing to note is the settling cavity that formed in the upper right hand part of the trap. Notice that it now contains trapped NAPL. Similar capillary trapping could occur within interface traps if coarse-grained zones are present.



## CHAPTER 4 – THE ROLE OF CAPILLARY FORCES IN NAPL TRAPPING: A CONCEPTUAL MODEL

Multiphase saturation of porous media is a function of the capillary pressure between the NAPL and the aqueous environment in a two-fluid porous medium system. The force, which is produced by pressure differences across the contact surfaces of the two different fluids, is called capillary pressure. In a two fluid system, when water is the wetting phase, capillary pressure,  $P_c$ , can be expressed as:

$$P_c = P_n - P_w = \frac{2\sigma \cos \theta}{\gamma} \quad (2)$$

Where  $P_n$  is the NAPL pressure,  $P_w$  is the water pressure,  $\sigma$  is the interfacial tension between the NAPL and water,  $\theta$  is the contact angle between the fluid surface (Fig. 14), and  $\gamma$  is the radius of water-filled pore. As  $\sigma$  increases, capillary pressure will increase. But  $P_c$  will decrease as  $\theta$  and  $\gamma$  increase.

The effect of wettability describes the preferential spreading of one fluid over a solid surface in a two-fluid system (Mercer and Cohen, 1990). It indicates that the wetting fluid will preferentially coat the grain surface and occupy the pore space in the pore medium relative to the nonwetting fluid. For two fluids, such as NAPL and water, in contact with a solid, the contact angle of the interface is described by (Fetter, 1993):

$$\cos \theta = \frac{\sigma_{NS} - \sigma_{WS}}{\sigma_{NW}} \quad (3)$$

Where  $\theta$  is the contact angle measured into the water,  $\sigma_{NS}$  is the interfacial tension between the NAPL and the solid,  $\sigma_{WS}$  is the interfacial tension between the water and the solid, and  $\sigma_{NW}$  is the interfacial tension between the NAPL and the water. The contact

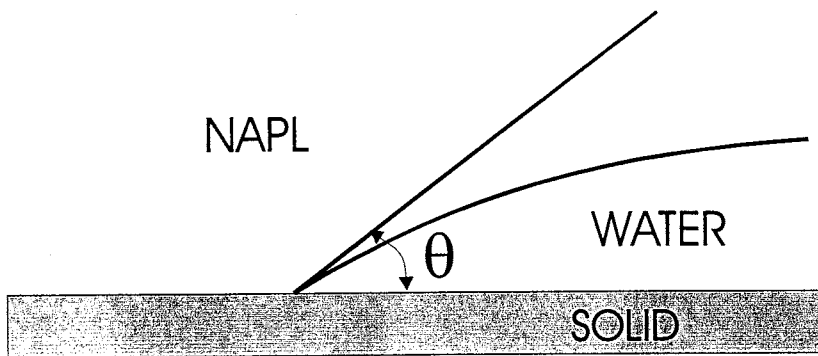


Figure 14. Definition of contact angle  $\theta$  (modified from Fetter, 1993).

angle varies between 0 and 180° and indicates whether NAPL or water will preferentially wet the porous medium. If  $\theta < 90^\circ$ , it indicates the tendency to be water-wet, but if  $\theta > 90^\circ$ , it tends to be NAPL wet.

Wettability relations in immiscible two-phase heterogeneous porous media are affected by factors such as NAPL chemistry, medium mineralogy, and porous medium saturation (Mercer and Cohen, 1990).

When a NAPL body is in contact with water in porous media, a capillary fringe or zone of capillarity exists between them (Levorsen, 1967). Water will intrude into the NAPL in the zone of capillarity until interfacial forces are balanced and it can no longer displace NAPL. The height of capillary rise for a given pore and pore throat size can be calculated from Hobson's Formula (Fetter, 1993; Berg, 1975).

$$h_c = \frac{2\sigma \cos \theta \left( \frac{1}{r_t} - \frac{1}{r_p} \right)}{(\rho_w - \rho_o)g} \quad (4)$$

Where  $h_c$  is the height of capillary rise in centimeters,  $\sigma$  is the interfacial tension between the NAPL and the water (dyne/cm),  $\theta$  is the contact angle measured through the wetting phase (water),  $r_t$  is the pore throat radius,  $r_p$  is the pore radius,  $g$  is the acceleration of gravity (980 cm/sec<sup>2</sup>),  $\rho_w$  is the density of water (g/cm<sup>3</sup>), and  $\rho_o$  is the density of oil (g/cm<sup>3</sup>). For well-sorted, well-rounded grains with rhombohedral packing and a diameter  $D$  (in cm),  $r_p \approx 0.212D$  and  $r_t \approx 0.077D$  (Fetter, 1993).

From Hobson's Formula, capillary pressure is related to the interfacial tension, contact angle and pore size. Because capillary pressure can restrict the movement of the NAPL into the water-saturated media, layers with small pores can serve as capillary

barriers to NAPL migration. In order to overcome the higher capillary pressure in the smaller pores; NAPL column height must increase to counteract the resistance to continued migration. The height of the NAPL column required to force entry into fine-grained barriers can be calculated by Equation 4 and is equal to  $h_c$ . Since capillary entry pressures are higher for finer-grained materials, finer-grained materials can trap larger columns of NAPL. Thus capillary forces control both NAPL entry into porous media, as well as the minimum closure required to trap a given NAPL due to the capillary rise of water into the NAPL body. For a trap to retain NAPL at above residual saturation, the closure must exceed the height of capillary rise of water into the NAPL.

## CHAPTER 5 - DISCUSSION

This study of the micro-scale topographic variation and measurement of closure volume at sand/shale interfaces is, apparently, the first of its kind and the results should not be interpreted as definitive. The purpose is to point out that such studies can and should be done, and to begin to investigate which topographic scales are important to study. The sand-box visualization experiments were done to illustrate the role of capillary pressure in NAPL trapping at sand/shale interfaces, and to see if potential trapping features, such as those I measured in the field, are likely to trap NAPLs.

As demonstrated in our sand-box experiments, for an interface trap to retain NAPLs, the closure height must be greater than the height of capillary rise of the water into the NAPL. In the first sand box experiment, which used 1.5 mm diameter glass beads, the 4 cm deep recess trapped oil and the zone of capillarity is less than 1 cm thick (Figure 10F). Hobson's Formula predicts a capillary height of 2.2 cm for Marvel Mystery Oil™ (density of 0.83 g/cm<sup>3</sup>, interfacial tension 24.3 dyne/cm, and contact angle 82°) for 1.5 mm diameter grains. Thus, Hobson's Formula predicts that our 4-cm deep trap should retain Marvel Mystery Oil™.

The 6.7 cm capillary height predicted for 0.5 mm grains indicates no oil would be trapped in the second box experiment (Figure 11F) and none was. The predicted 16.8 cm capillary rise for 0.2 mm diameter grains compares favorably with the results of experiments 3 and 4. With a capillary rise of 16.8 cm, no oil should be trapped in a 4-cm high trap, and none was. Thus, comparison of the results of our visualization experiments with calculations made using Hobson's Formula suggest that it is

reasonably accurate, as did Berg's (1975) evaluation of Hobson's Formula applied to oil field data.

Some example calculations with Equation 4 iterated over grain-size for different NAPLs will help us illustrate the scale at which interface NAPL trapping is likely. Benzene, an LNAPL, with a density of 0.8737 and an interfacial tension of 35.0 dynes/cm, is a common contaminant (Fetter, 1993). The height of capillary rise of water into benzene for the range of  $\theta$  reported in Mercer and Cohen (1990) ranges from between 15 and 19.6 cm for a 2-mm grain-size (granules) to between 4.8 and 6.3 m for a grain-size of 0.0625 mm (0.0625 mm is the boundary between very fine grained sand and silt) (Fig. 15). Trap closure height must be greater than the height of capillary rise of water into the NAPL for a given aquifer grain size in order for the trap to retain the NAPL at above residual saturation. In order for benzene to be trapped at sand/shale interfaces, trap closure heights must be in excess of 15 cm to more than 6.3 m, depending upon the grain-size within the trapping structure.

This relation is consistent when applied to diesel fuels (Figure 16). Benzene and diesel fuels have similar density values, but the diesel fuel's interfacial tension is 1.4 times larger than that of benzene so it will have a higher capillary rise than that of benzene with the same contact angle. For diesel fuels in 2mm-sized material, capillarity is between 15 and 20 cm. (Fig. 16). For sands at the very fine-grained sand/silt boundary, the needed closure height for diesel fuels increase to between 5.0 and 6.5 meters. Therefore, greater closure height should be required to trap diesel fuels than benzene.

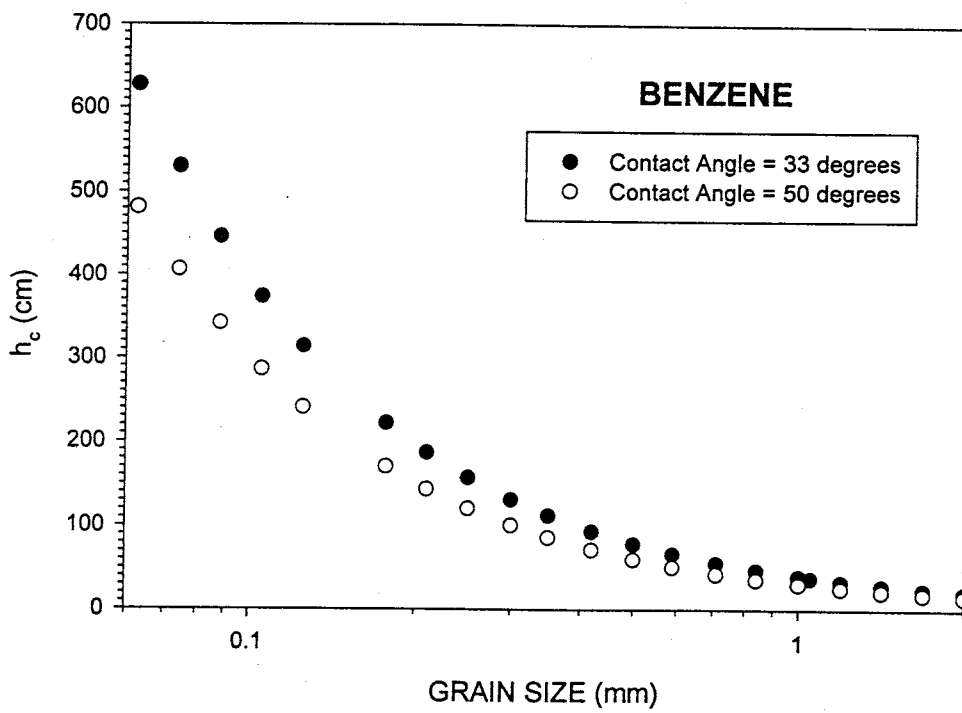


Figure 15. Relation of height of capillary rise of water in to benzene versus grain-size of aquifer matrix.

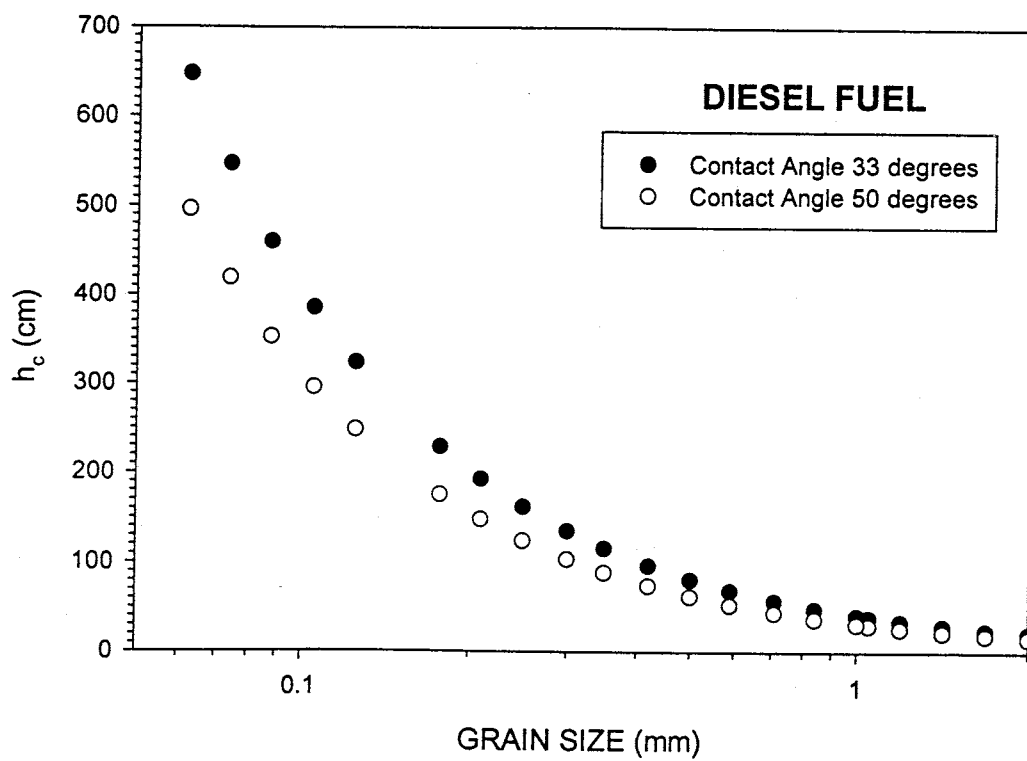


Figure 16. Relation of height of capillary rise of water in to diesel fuel versus grain-size of aquifer matrix.



For DNAPL, capillarity forces water into the DNAPL body in a downward direction, thus the calculated height of capillary rise is negative. Therefore, in Figures 17 and 18 we plotted the absolute value of capillary rise for DNAPLs to facilitate comparison between LNAPLs and DNAPLs. Dichloromethane and trichloromethane both are DNAPLs. Both have a similar density, but trichloromethane has interfacial tension 1.1 times larger than dichloromethane resulting in a higher capillary rise. This comparison indicates that as the interfacial tension increases the capillary pressure increases also. To trap dichloromethane requires a closure height between 4.5 and 8.5 cm for 2-mm sized material (Fig. 17) the necessary closure height rises to between 1.47 and 1.9 m for well-sorted very fine-grained sand (0.0625 mm diameter). For trichloromethane (Figure 18), the height of capillarity for well-sorted 2-mm granules is between 3.5 and 4.7 cm. For very fine-grained sand (0.0625 mm diameter) it rises to between 1.14 and 1.49 meters.

From Figures 15, 16, 17, and 18 and examination of Equation 4, we develop some general conclusions:

1. For LNAPLs and DNAPLs, the closer the immiscible fluid density is to that of water, the greater the capillary rise and therefore, the greater the closure height necessary to retain the NAPL in an interface trap.
2. Because DNAPLs have a greater range of density, smaller closure heights should be efficient to trap some denser DNAPLs than are needed to trap common LNAPLs.

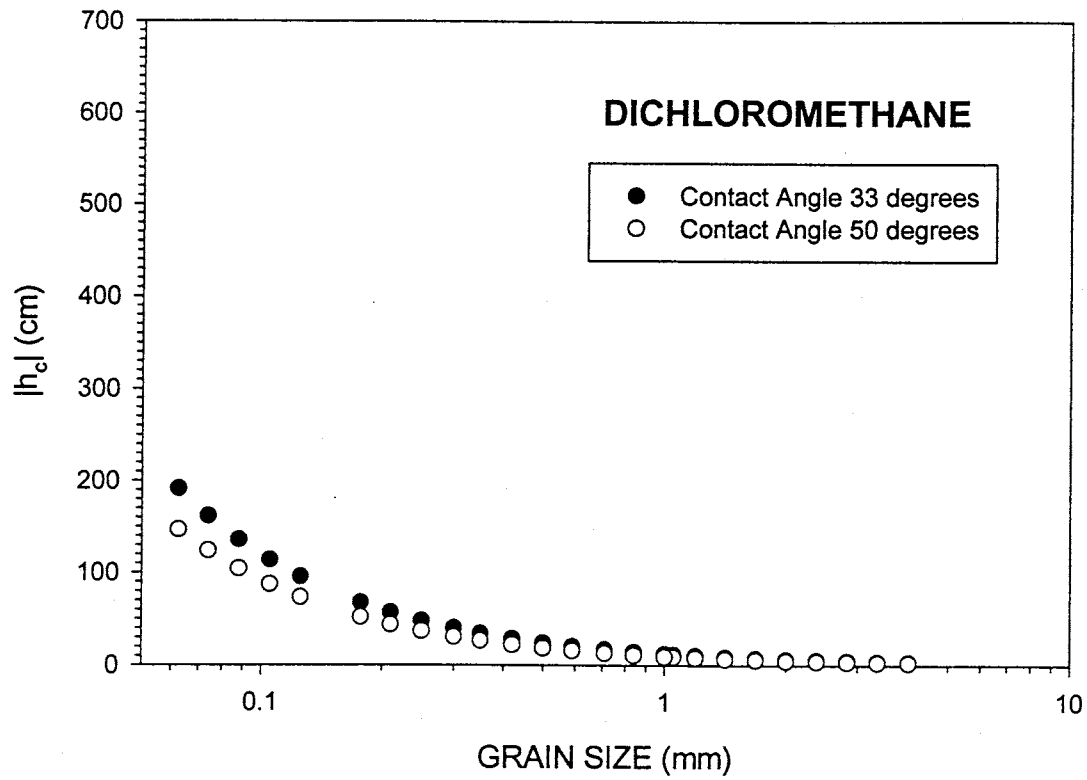


Figure 17. Relation of height of capillary rise of water in to dichloromethane versus grain-size of aquifer matrix.

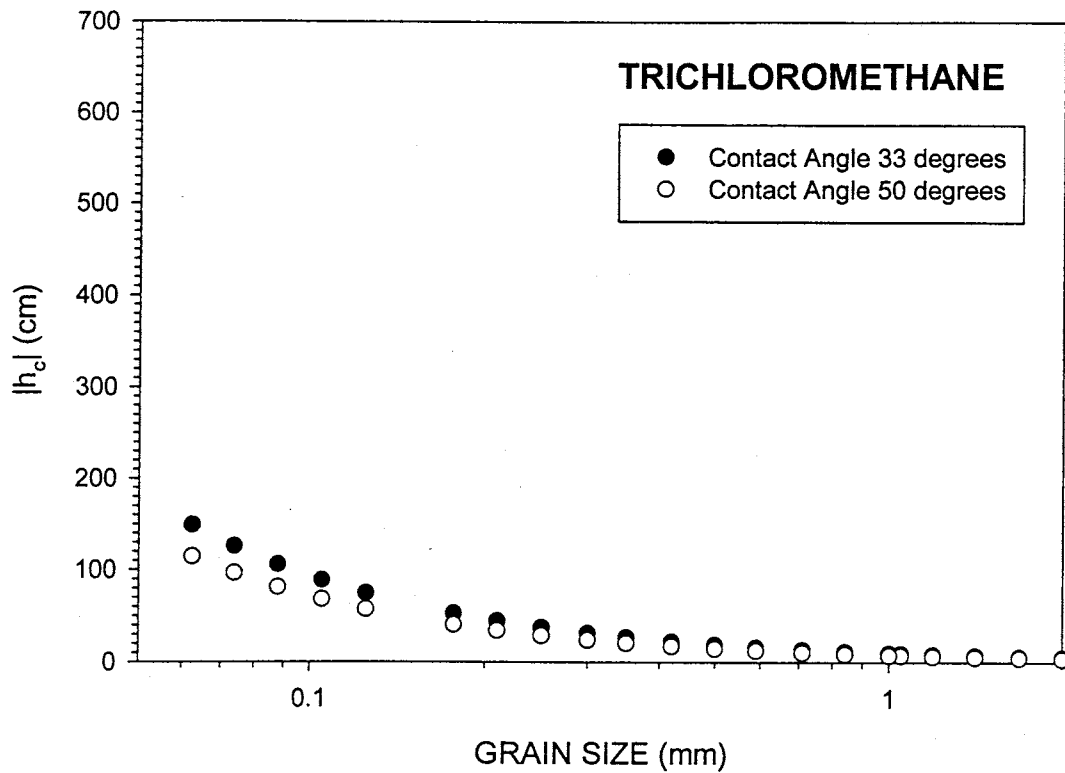


Figure 18. Relation of height of capillary rise of water in to trichloromethane versus grain-size of aquifer matrix.

3. In all cases the height of capillarity is inversely proportional to the grain-size in the trap. Therefore, it becomes necessary to know grain-size distributions and sorting at contaminated sites as well as interface geometry in order to predict the potential importance of interface trapping.

Grain sorting is potentially important with respect to Hobson's Formula.

Because the  $r_p$  and  $r_t$  parameters are based on an approximation of rhombohedral packing of uniform spheres (Berg, 1975), Hobson's Formula should predict behavior in well-sorted sands reasonably well. However, in a poorly-sorted sand, which consists of a wide mix of grain sizes, the smaller grains fill in the spaces between the larger grains. Therefore, the pores and pore throats associated with the smaller grains control capillarity. Consequently, poorly-sorted sands may behave like finer-grained material than the mean grain size might suggest.

Hubbert (1953) derived an equation that describes the tilt of an oil/water contact due to the density difference between the water and the oil and the groundwater head gradient. This equation is

$$\tan \tau = \frac{\rho_w}{\rho_w - \rho_o} \frac{dh}{dl} \quad (5)$$

Where  $\tau$  is the angle between the horizontal and the oil/water interface,  $\rho_w$  is the density of the water,  $\rho_o$  is the density of the oil, and  $dh/dl$  is the groundwater gradient.

Groundwater gradients in natural systems generally range from less than 0.0001 (less than 1 foot per mile) to 0.02 (about 100 feet per mile). Therefore, for an LNAPL of density 0.8,  $\tau$  will range between  $0.029^\circ$  for a gradient of 0.0001 and  $5.7^\circ$  for a gradient

of 0.02. Equation 5 states that the sensitivity factor ( $\rho_w/\rho_w-\rho_o$ ) increases as the density of the oil approaches the density of water. Therefore, for benzene (density 0.87 g/cm<sup>3</sup>)  $\tau$  will range between 0.044° for a gradient of 0.0001 and 8.75° for a gradient of 0.02. These calculations suggest that significant angles  $\tau$  will only develop where groundwater gradients are relatively steep.

In sandbox experiment 1, the angle between the horizontal and the oil water contact (Figure 10F) at the end of our experiment is approximately 15°. Equation 5 suggests that for our high experimental gradient (0.97) that  $\tau$  should be 80.2°. Two possible reasons exist for the difference in the observed angle and the angle calculated from equation 5: 1) the equation is not accurate for very high gradients such as used in the experiment, or 2) the experiment was not yet at steady state.

The investigation of closure volume and topographic variation at sand shale interfaces demonstrated that there is potential for significant trapping volumes to exist at interfaces at the micro-scale. Even interfaces which have relief of only a few centimeters can generate closure volumes of more than 1.2 L/m<sup>2</sup> (which assuming a porosity of 30 percent yields trapping volumes of 0.36 L/m<sup>2</sup> or more). However, as the sand-box experiments and calculations have shown, closure heights of only a few centimeters are significant only when the grain-size is quite coarse. Coarse sands and gravels do exist at interfaces, however, so this is a potentially important observation.

Features in intermontane basins which might form environmentally significant NAPL traps include alluvial fan, fluvial, lacustrine, eolian, biogenic, pedogenic, volcanic, and tectonic features (Love et al., 1997). Future studies of these features with

respect to potential NAPL trap closure height, volume, grain size parameters, and distribution may lead to better quantification of NAPL-trapping features. One of the most significant problems in site investigation is the scale at which a site can be examined. It is seldom cost-effective to take borings spaced less than a few meters apart. Thus, with soil borings, only relatively large scale NAPL traps might be detected. Therefore, high resolution seismic techniques, electromagnetic techniques, or ground-penetrating radar, with vertical resolutions which approach one meter (Reynolds, 1997) show promise in detecting the presence of smaller-scale NAPL traps at contaminated sites. Reynolds (1997) has presented a thorough, environmentally-oriented overview of various geophysical techniques for the reader who wishes to pursue this subject further. The fact that relatively small-scale traps might be important at some NAPL contaminated sites points out the need for further research into micro-scale geophysical techniques which will allow noninvasive, three-dimensional delineation of the petrophysical properties of contaminated aquifers on a scale of tens of centimeters or less.

Although high-resolution geophysical techniques may someday delineate subsurface strata at adequate scales for effective, non-invasive site investigation, it is likely that a detailed understanding of permeability pathways and NAPL trapping processes will be needed to design remediation efforts. Thus geological studies of NAPL trapping processes and the permeability structure of potential NAPL traps may contribute to future remediation of NAPL contaminated sites.

## CHAPTER 6 - SUMMARY AND CONCLUSIONS

Just as oil and gas are trapped in the subsurface, NAPLs can be trapped by smaller scale features with adequate closure at sand/shale interfaces. LNAPLs are less dense than water and tend to collect either at the water table or along the upper bounding surface of a confined aquifer where they can be trapped. DNAPLs are denser than water and migrate to lower aquifer boundaries where they also can be trapped.

Micro-scale closure volumes were measured at the upper sand/shale interface for 62 locations at three sites for fluvial/alluvial and tidal flat depositional environments and I found that closure volume ranged from a low of  $0.56 \text{ L/m}^2$  to a high of  $2.88 \text{ L/m}^2$ . The average for all sites was  $1.22 \text{ L/m}^2$ . The area of each site ranged between  $1024$  and  $2090 \text{ cm}^2$ . The closure height for individual features could not be measured, so we measured the topographic variation at each location. Topographic variation ranged up to a maximum of  $3.3 \text{ cm}$ , and site means ranged between  $1.3$  and  $2.4 \text{ cm}$ .

Sand-box experiments were also conducted to see if micro-scale features have NAPL trapping potential. The results suggest that for NAPL to be trapped at greater than residual saturation, the closure height must be greater than the capillary rise of water into the NAPL. A closure height of  $4.0 \text{ cm}$  effectively trapped Marvel Mystery Oil™ when the average grain size was  $1.5 \text{ mm}$ , but failed to do so at smaller grain-sizes.

The results of the sand box visualization experiments and calculations with Hobson's Formula suggest that trap closure heights in the saturated zone must exceed the thickness of the zone of water capillarity before NAPL can be trapped at greater than residual saturation. Capillary heights are a function of both grain size and the physical properties of the specific NAPL compound. For coarse-sized material, capillary heights

are generally on the order of one to a few centimeters. For fine-grained sands, capillary heights are on the order of nearly one meter to as much as five meters or more. This suggests that trapping features containing coarse-grained material can retain NAPL at greater than residual saturation when closure heights are less than 10 cm. However, traps containing fine-grained sands, depending upon the specific NAPL compound, need closure heights on the order of one to five meters or more to trap NAPL. Thus, the micro-scale features we examined can only act as significant NAPL traps when the grain-size within the trap is quite coarse.

From our sand-box experiments, a closure height of 4.0 cm could trap Marvel Mystery Oil™ when the average grain size was 1.5 mm, but failed at smaller grain-sizes. From our field work, the mean value of the topographic variation varied between 2.4 to 4.8 cm for the three sites. Comparing the laboratory and field results indicates that small scale trapping did exist and play an important role.

For both LNAPLs and DNAPLs, the closer the fluid density is to that of water, the greater the capillary rise, and therefore the greater the closure height necessary to retain the NAPL in an interface trap. NAPLs having densities differing greatly from that of water require the least closure to trap. In all cases the height of capillarity is inversely proportional to grain-size. Therefore, it becomes necessary to know grain-size distribution and sorting as well as interface geometry in order to predict the potential importance of interface trapping at contaminated sites.

Future work could include quantifying the closure volume distribution of the micro-scale features by geostatistical analysis. If such a geostatistical predictive model



can be developed, the NAPL trapping potential of sand/shale interfaces in the depositional environment can be determined.

## REFERENCES CITED

- Berg, R. R., 1975. Capillary pressure in stratigraphic traps. American Association of Petroleum Geologists Bulletin, 59, No. 6, p.939-956.
- Chamberlin, R. M., 1980, Cenozoic stratigraphy and structure of the Socorro Peak volcanic center, central New Mexico, New Mexico Bureau of Mines and mineral Resources Open File Report 118, 2 vols, 495 p.
- Chamberlin, R. M., 1981, Cenozoic stratigraphy and structure of the Socorro Peak volcanic center, central New Mexico. A summary. New Mexico Geology, v. 3, no. 2, p. 22-24.
- Cohen, R. M. and Mercer, J. W., 1993. DNAPL Site Evaluation, C. K. Smoley, Publisher, CRC Press, Boca Raton, 339 p.
- Dahlberg, E. C., 1995. Applied Hydrodynamics in Petroleum Exploration, 2nd ed., Springer Verlag, New York, 295 p.
- Feenstra, S. and Coburn, J., 1986. Subsurface contamination from spills of denser than water chlorinated solvents. California Water Pollution Control Association Bulletin 23: 26-34.
- Fetter, C. W., 1993. Contaminant Hydrogeology. MacMillian Publishing Company, New York, 458p.
- Hubbert, M. K., 1953, Entrapment of petroleum under hydrodynamic conditions, Bulletin of the American Association of Petroleum Geologists, V. 37, pp 1954-2026.
- Levorsen, A. I., 1967. Geology of Petroleum, W. H. Freeman and Company, San Francisco, 724p.
- Love, D. W., Whitworth, T. M., Seager, W. R., and Davis, J. M., 1997. Possible NAPL trapping features in semiarid-basin fill (abstract), Symposium no. 5, Environmental Geology and Hydrology of Intermontane Basins" for the South-Central/Rocky Mountain GSA Joint Meeting March 1997.
- Mack, G. H. and Suguio, K., 1991, Depositional environments of the Yeso Formation (lower Permian), southern Caballo Mountains, New Mexico, New Mexico Geology, Vol. 13, No. 3, p. 45-49.
- Mercer, J.W. and Cohen, R. M., 1990. A review of immiscible fluids in the subsurface: Properties, models, characterization, and remediation. Journal of Contaminant Hydrogeology, 6: 107-163.

- Meyer, H. W., 1983, Fossil Plants from the early Neogene Socorro flora, central New Mexico, New Mexico Geological Society Guidebook, 34<sup>th</sup> field conference, Socorro Region II, p. 193-196.
- Palmer, C. M., 1992. Principles of Contaminant Hydrogeology, Lewis Publishers, Boca Raton, 211 p.
- Pinder, G. F., and Abriola, L., 1986. On the simulation of nonaqueous phase organic compounds in the subsurface. *Water Resources Research* 22: 109S-119S.
- Reynolds, J. M., 1997. An introduction to applied and environmental geophysics. John Wiley & Sons, New York, 796p.
- Schroth, M. H., Istok, J. D., Ahearn, S. J., and Selker, J. S., 1995. Geometry and position of light nonaqueous-phase liquid lenses in water-wetted porous media. *Journal of Contaminant Hydrology*, 19: 269-287.
- Titus, F. B., 1963, Geology and ground-water conditions in eastern Valencia county, New Mexico, New Mexico Bureau of Mines and mineral Resources Ground-Water Report 7, 113 p.
- Van Geel, P. J., and Sykes, J. F., 1994. Laboratory and model simulations of a LNAPL spill in a variably-saturated sand, 1. Laboratory experiment and image analysis techniques. *Journal of Contaminant Hydrology*, 17: 1-25.
- Vroblesky, C. D., Robertson, J. F., and Rhodes, L. C., 1995. Stratigraphic trapping of spilled jet fuel beneath the water table. *Groundwater Monitoring Review*, Spring Volume, 177-183.
- Whitworth, T. M., 1994. Possible impact of shallow traps on groundwater remediation. *Environmental Geology*, 23: 30-35.
- Zalidis, G. C., Annable, M. D., Wallace, R. B., Hayden, N. J., and Voice, T. C., 1991. A laboratory method for studying the aqueous phase transport of dissolved constituents from residually held NAPL in unsaturated soil columns. *Journal of Contaminant Hydrology*, 8: 143-156.

## APPENDIX A: SITE INFORMATION

### SITE 1

Location: Socorro, County, NM. Latitude: 34° 09'81" N, Longitude: 106° 45'00".

Elevation: 5096 feet.

Age: Permian

Formation: Yeso

Depositional Environment: Tidal Flat.

### SITE 2

Location: Socorro, County, NM. Latitude: 34° 09'84" N, Longitude: 106° 45'00".

Elevation: 5110 feet.

Age: Permian

Formation: Yeso

Depositional Environment: Playa Lake/Aeolian Sand

### SITE 3

Location: Socorro, County, NM. Latitude: 34° 13'50" N, Longitude: 106° 59'06".

Elevation: 4650 feet.

Age: Miocene

Formation: Popotosa

Depositional Environment: Distal alluvial fan/fluvial

## APPENDIX B: SAND/SHALE INTERFACE CLOSURE DATA

### SITE 1 SUMMARY DATA

Location: Latitude 34°09'81" N, Longitude 106°45'00"  
 Elevation: 5096 feet.

Sample No.	Closure volume (cm <sup>3</sup> )	Frame area (cm <sup>2</sup> )	Standard Deviation (%)
2-21-97-1	94.803	1024.00	1.30
2-21-97-2	98.627	1024.00	3.60
2-21-97-3	143.700	1024.00	2.10
2-21-97-4	128.337	1024.00	0.70
2-21-97-5	114.657	1024.00	1.50
2-21-97-6	105.980	1024.00	0.60
2-21-97-7	109.490	1024.00	1.40
2-21-97-8	136.003	1024.00	0.90
2-21-97-9	115.230	1024.00	2.50
2-21-97-10	147.210	1024.00	1.60
2-21-97-11	116.923	1024.00	1.50
2-21-97-12	70.307	1024.00	2.30
2-21-97-13	169.090	1024.00	1.20
2-21-97-14	103.827	1024.00	1.00
2-21-97-15	123.510	1024.00	0.70
2-21-97-16	106.547	1024.00	0.90
2-21-97-17	77.930	1024.00	0.50
2-21-97-18	119.617	1024.00	2.40
2-21-97-19	69.913	1024.00	3.60
2-21-97-20	146.910	1024.00	4.10
2-21-97-21	104.063	1024.00	0.80

Closure Volume Statistics						
n	Mean	Std. Dev.	Std. Error	Range	Maximum	Minimum
21	114.413	25.517	5.568	99.177	169.090	69.913
Standard Deviation Statistics						
n	Mean	Std. Dev.	Std. Error	Range	Maximum	Minimum
21	1.676	1.059	0.231	3.600	4.100	0.500

Sample No.	Closure volume (cm <sup>3</sup> )	Frame area (cm <sup>2</sup> )	Standard Deviation (%)
5-19-97-1	131.703	1451.61	2.55
5-19-97-2	138.327	1451.61	2.62
5-19-97-3	151.577	1451.61	2.42
5-19-97-4	189.857	1451.61	0.80
5-19-97-5	225.027	1451.61	1.35
5-19-97-6	152.690	1451.61	1.82
5-19-97-7	188.357	1451.61	1.89
5-19-97-8	192.370	1451.61	1.27
5-19-97-9	178.867	1451.61	1.14
5-19-97-10	196.033	1451.61	2.18

Closure Volume Statistics						
n	Mean	Std. Dev.	Std. Error	Range	Maximum	Minimum
10	174.481	29.672	9.383	93.324	225.027	131.703
Standard Deviation Statistics						
n	Mean	Std. Dev.	Std. Error	Range	Maximum	Minimum
10	1.804	0.640	0.203	1.820	2.620	0.800

Sample No.	Closure volume (cm <sup>3</sup> )	Frame area (cm <sup>2</sup> )	Standard Deviation (%)
6-11-97-1	244.220	2090.32	1.00
6-11-97-2	239.837	2090.32	1.66
6-11-97-3	237.983	2090.32	0.86
6-11-97-4	204.943	2090.32	1.17
6-11-97-5	265.237	2090.32	0.90
6-11-97-6	214.897	2090.32	1.10
6-11-97-7	308.507	2090.32	1.35
6-11-97-8	252.540	2090.32	1.63
6-11-97-9	212.000	2090.32	0.83
6-11-97-10	220.773	2090.32	1.50

Closure Volume Statistics						
n	Mean	Std. Dev.	Std. Error	Range	Maximum	Minimum
10	240.094	30.772	9.731	103.564	308.507	204.943
Standard Deviation Statistics						
n	Mean	Std. Dev.	Std. Error	Range	Maximum	Minimum
10	1.200	0.317	0.100	0.830	1.660	0.830

SITE 1 RAW DATA

Sample No.	Closure volume (cm <sup>3</sup> )	Frame area (cm <sup>2</sup> )
2-21-97-1	101.36	1024.00
2-21-97-1	93.36	1024.00
2-21-97-1	95.75	1024.00
2-21-97-1	95.30	1024.00
Sample No.	Closure volume (cm <sup>3</sup> )	Frame area (cm <sup>2</sup> )
2-21-97-2	121.24	1024.00
2-21-97-2	102.64	1024.00
2-21-97-2	96.07	1024.00
2-21-97-2	97.17	1024.00
Sample No.	Closure volume (cm <sup>3</sup> )	Frame area (cm <sup>2</sup> )
2-21-97-3	161.40	1024.00
2-21-97-3	145.95	1024.00
2-21-97-3	144.94	1024.00
2-21-97-3	140.21	1024.00
Sample No.	Closure volume (cm <sup>3</sup> )	Frame area (cm <sup>2</sup> )
2-21-97-4	159.10	1024.00
2-21-97-4	129.29	1024.00
2-21-97-4	128.35	1024.00
2-21-97-4	127.37	1024.00
Sample No.	Closure volume (cm <sup>3</sup> )	Frame area (cm <sup>2</sup> )
2-21-97-5	134.05	1024.00
2-21-97-5	115.36	1024.00
2-21-97-5	112.72	1024.00
2-21-97-5	115.89	1024.00
Sample No.	Closure volume (cm <sup>3</sup> )	Frame area (cm <sup>2</sup> )
2-21-97-6	106.50	1024.00
2-21-97-6	105.86	1024.00
2-21-97-6	105.28	1024.00
2-21-97-6	106.16	1024.00
Sample No.	Closure volume (cm <sup>3</sup> )	Frame area (cm <sup>2</sup> )
2-21-97-7	133.27	1024.00
2-21-97-7	107.99	1024.00
2-21-97-7	109.47	1024.00
2-21-97-7	111.01	1024.00

Sample No.	Closure volume (cm <sup>3</sup> )	Frame area (cm <sup>2</sup> )
2-21-97-8	171.33	1024.00
2-21-97-8	137.31	1024.00
2-21-97-8	135.89	1024.00
2-21-97-8	134.81	1024.00
Sample No.	Closure volume (cm <sup>3</sup> )	Frame area (cm <sup>2</sup> )
2-21-97-9	117.57	1024.00
2-21-97-9	115.77	1024.00
2-21-97-9	116.14	1024.00
2-21-97-9	111.98	1024.00
Sample No.	Closure volume (cm <sup>3</sup> )	Frame area (cm <sup>2</sup> )
2-21-97-10	158.40	1024.00
2-21-97-10	149.76	1024.00
2-21-97-10	145.13	1024.00
2-21-97-10	146.74	1024.00
Sample No.	Closure volume (cm <sup>3</sup> )	Frame area (cm <sup>2</sup> )
2-21-97-11	126.29	1024.00
2-21-97-11	116.70	1024.00
2-21-97-11	118.78	1024.00
2-21-97-11	115.29	1024.00
Sample No.	Closure volume (cm <sup>3</sup> )	Frame area (cm <sup>2</sup> )
2-21-97-12	82.29	1024.00
2-21-97-12	72.07	1024.00
2-21-97-12	69.98	1024.00
2-21-97-12	68.87	1024.00
Sample No.	Closure volume (cm <sup>3</sup> )	Frame area (cm <sup>2</sup> )
2-21-97-13	171.46	1024.00
2-21-97-13	168.22	1024.00
2-21-97-13	168.09	1024.00
2-21-97-13	167.72	1024.00
Sample No.	Closure volume (cm <sup>3</sup> )	Frame area (cm <sup>2</sup> )
2-21-97-14	113.45	1024.00
2-21-97-14	103.91	1024.00
2-21-97-14	104.78	1024.00
2-21-97-14	102.79	1024.00
Sample No.	Closure volume (cm <sup>3</sup> )	Frame area (cm <sup>2</sup> )
2-21-97-15	125.22	1024.00
2-21-97-15	124.33	1024.00
2-21-97-15	123.63	1024.00
2-21-97-15	122.57	1024.00



Sample No.	Closure volume (cm <sup>3</sup> )	Frame area (cm <sup>2</sup> )
2-21-97-16	107.59	1024.00
2-21-97-16	96.59	1024.00
2-21-97-16	105.62	1024.00
2-21-97-16	106.43	1024.00
Sample No.	Closure volume (cm <sup>3</sup> )	Frame area (cm <sup>2</sup> )
2-21-97-17	83.59	1024.00
2-21-97-17	77.54	1024.00
2-21-97-17	77.94	1024.00
2-21-97-17	78.31	1024.00
Sample No.	Closure volume (cm <sup>3</sup> )	Frame area (cm <sup>2</sup> )
2-21-97-18	119.52	1024.00
2-21-97-18	116.79	1024.00
2-21-97-18	122.54	1024.00
2-21-97-18	84.17	1024.00
Sample No.	Closure volume (cm <sup>3</sup> )	Frame area (cm <sup>2</sup> )
2-21-97-19	72.81	1024.00
2-21-97-19	68.82	1024.00
2-21-97-19	68.11	1024.00
2-21-97-19	71.15	1024.00
Sample No.	Closure volume (cm <sup>3</sup> )	Frame area (cm <sup>2</sup> )
2-21-97-20	153.68	1024.00
2-21-97-20	142.59	1024.00
2-21-97-20	144.80	1024.00
2-21-97-20	142.25	1024.00
Sample No.	Closure volume (cm <sup>3</sup> )	Frame area (cm <sup>2</sup> )
2-21-97-21	127.09	1024.00
2-21-97-21	98.37	1024.00
2-21-97-21	99.45	1024.00
2-21-97-21	99.96	1024.00
Sample No.	Closure volume (cm <sup>3</sup> )	Frame area (cm <sup>2</sup> )
5-19-97-1	135.46	1451.61
5-19-97-1	133.11	1451.61
5-19-97-1	129.01	1451.61
5-19-97-1	130.64	1451.61
Sample No.	Closure volume (cm <sup>3</sup> )	Frame area (cm <sup>2</sup> )
5-19-97-2	142.11	1451.61
5-19-97-2	134.88	1451.61
5-19-97-2	137.99	1451.61
5-19-97-2	139.96	1451.61
5-19-97-3	162.71	1451.61

5-19-97-3	148.76	1451.61
5-19-97-3	150.24	1451.61
5-19-97-3	155.73	1451.61
Sample No.	Closure volume (cm <sup>3</sup> )	Frame area (cm <sup>2</sup> )
5-19-97-4	191.18	1451.61
5-19-97-4	190.19	1451.61
5-19-97-4	185.36	1451.61
5-19-97-4	188.20	1451.61
Sample No.	Closure volume (cm <sup>3</sup> )	Frame area (cm <sup>2</sup> )
5-19-97-5	228.43	1451.61
5-19-97-5	222.57	1451.61
5-19-97-5	203.65	1451.61
5-19-97-5	224.08	1451.61
Sample No.	Closure volume (cm <sup>3</sup> )	Frame area (cm <sup>2</sup> )
5-19-97-6	154.65	1451.61
5-19-97-6	128.20	1451.61
5-19-97-6	150.73	1451.61
5-19-97-6	146.32	1451.61
Sample No.	Closure volume (cm <sup>3</sup> )	Frame area (cm <sup>2</sup> )
5-19-97-7	192.22	1451.61
5-19-97-7	182.35	1451.61
5-19-97-7	192.22	1451.61
5-19-97-7	187.62	1451.61
Sample No.	Closure volume (cm <sup>3</sup> )	Frame area (cm <sup>2</sup> )
5-19-97-8	131.00	1451.61
5-19-97-8	192.78	1451.61
5-19-97-8	189.75	1451.61
5-19-97-8	194.58	1451.61
Sample No.	Closure volume (cm <sup>3</sup> )	Frame area (cm <sup>2</sup> )
5-19-97-9	142.51	1451.61
5-19-97-9	176.70	1451.61
5-19-97-9	179.17	1451.61
5-19-97-9	180.73	1451.61
Sample No.	Closure volume (cm <sup>3</sup> )	Frame area (cm <sup>2</sup> )
5-19-97-10	156.30	1451.61
5-19-97-10	198.60	1451.61
5-19-97-10	191.10	1451.61
5-19-97-10	198.40	1451.61

Sample No.	Closure volume (cm <sup>3</sup> )	Frame area (cm <sup>2</sup> )
6-11-97-1	249.52	2090.32
6-11-97-1	241.50	2090.32
6-11-97-1	246.16	2090.32
6-11-97-1	245.00	2090.32
Sample No.	Closure volume (cm <sup>3</sup> )	Frame area (cm <sup>2</sup> )
6-11-97-2	257.63	2090.32
6-11-97-2	235.61	2090.32
6-11-97-2	240.36	2090.32
6-11-97-2	243.54	2090.32
Sample No.	Closure volume (cm <sup>3</sup> )	Frame area (cm <sup>2</sup> )
6-11-97-3	246.52	2090.32
6-11-97-3	240.29	2090.32
6-11-97-3	237.24	2090.32
6-11-97-3	236.42	2090.32
Sample No.	Closure volume (cm <sup>3</sup> )	Frame area (cm <sup>2</sup> )
6-11-97-4	167.66	2090.32
6-11-97-4	202.43	2090.32
6-11-97-4	205.20	2090.32
6-11-97-4	207.20	2090.32
Sample No.	Closure volume (cm <sup>3</sup> )	Frame area (cm <sup>2</sup> )
6-11-97-5	269.39	2090.32
6-11-97-5	265.18	2090.32
6-11-97-5	267.64	2090.32
6-11-97-5	262.89	2090.32
Sample No.	Closure volume (cm <sup>3</sup> )	Frame area (cm <sup>2</sup> )
6-11-97-6	249.91	2090.32
6-11-97-6	213.97	2090.32
6-11-97-6	217.59	2090.32
6-11-97-6	213.13	2090.32
Sample No.	Closure volume (cm <sup>3</sup> )	Frame area (cm <sup>2</sup> )
6-11-97-7	267.09	2090.32
6-11-97-7	303.86	2090.32
6-11-97-7	311.87	2090.32
6-11-97-7	309.79	2090.32
Sample No.	Closure volume (cm <sup>3</sup> )	Frame area (cm <sup>2</sup> )
6-11-97-8	217.17	2090.32
6-11-97-8	248.98	2090.32
6-11-97-8	257.04	2090.32
6-11-97-8	251.60	2090.32

Sample No.	Closure volume (cm <sup>3</sup> )	Frame area (cm <sup>2</sup> )
6-11-97-9	205.99	2090.32
6-11-97-9	213.92	2090.32
6-11-97-9	211.63	2090.32
6-11-97-9	210.45	2090.32
Sample No.	Closure volume (cm <sup>3</sup> )	Frame area (cm <sup>2</sup> )
6-11-97-10	218.21	2090.32
6-11-97-10	223.32	2090.32
6-11-97-10	221.98	2090.32
6-11-97-10	217.02	2090.32

### SITE 2 SUMMARY DATA

Location: Latitude 34°09'84" N, Longitude 106°45'00" E  
Elevation: 5110 feet

Sample No.	Closure volume (cm <sup>3</sup> )	Frame area (cm <sup>2</sup> )	Standard Deviation (%)
3-21-97-1	91.637	1024.00	1.12
3-21-97-2	95.873	1024.00	1.30
3-21-97-3	98.457	1024.00	0.90
3-21-97-4	294.623	1024.00	0.80
3-21-97-5	285.112	1024.00	1.36
3-21-97-6	107.653	1024.00	1.87
3-21-97-7	168.547	1024.00	1.53
3-21-97-8	227.390	1024.00	1.07
3-21-97-9	56.787	1024.00	1.92
3-21-97-10	129.553	1024.00	1.28
3-21-97-11	74.290	1024.00	1.23
3-21-97-12	124.723	1024.00	1.29

Closure Volume Statistics						
n	Mean	Std. Dev.	Std. Error	Range	Maximum	Minimum
12	146.220	80.677	23.289	237.836	294.623	56.787
Standard Deviation Statistics						
n	Mean	Std. Dev.	Std. Error	Range	Maximum	Minimum
12	1.306	0.339	0.0979	1.120	1.920	0.800

SITE 2 RAW DATA

Sample No.	Closure volume (cm <sup>3</sup> )	Frame area (cm <sup>2</sup> )
3-21-97-1	92.81	1024.00
3-21-97-1	90.90	1024.00
3-21-97-1	91.53	1024.00
3-21-97-1	91.20	1024.00
Sample No.	Closure volume (cm <sup>3</sup> )	Frame area (cm <sup>2</sup> )
3-21-97-2	92.49	1024.00
3-21-97-2	95.91	1024.00
3-21-97-2	97.10	1024.00
3-21-97-2	94.61	1024.00
Sample No.	Closure volume (cm <sup>3</sup> )	Frame area (cm <sup>2</sup> )
3-21-97-3	98.69	1024.00
3-21-97-3	97.66	1024.00
3-21-97-3	98.30	1024.00
3-21-97-3	99.41	1024.00
Sample No.	Closure volume (cm <sup>3</sup> )	Frame area (cm <sup>2</sup> )
3-21-97-4	292.77	1024.00
3-21-97-4	297.42	1024.00
3-21-97-4	293.68	1024.00
3-21-97-4	297.75	1024.00
Sample No.	Closure volume (cm <sup>3</sup> )	Frame area (cm <sup>2</sup> )
3-21-97-5	288.72	1024.00
3-21-97-5	287.80	1024.00
3-21-97-5	280.46	1024.00
3-21-97-5	283.51	1024.00
Sample No.	Closure volume (cm <sup>3</sup> )	Frame area (cm <sup>2</sup> )
3-21-97-6	102.30	1024.00
3-21-97-6	105.33	1024.00
3-21-97-6	108.75	1024.00
3-21-97-6	108.88	1024.00
Sample No.	Closure volume (cm <sup>3</sup> )	Frame area (cm <sup>2</sup> )
3-21-97-7	168.79	1024.00
3-21-97-7	166.42	1024.00
3-21-97-7	167.80	1024.00
3-21-97-7	171.41	1024.00

Sample No.	Closure volume (cm <sup>3</sup> )	Frame area (cm <sup>2</sup> )
3-21-97-8	205.24	1024.00
3-21-97-8	226.63	1024.00
3-21-97-8	230.11	1024.00
3-21-97-8	225.43	1024.00
Sample No.	Closure volume (cm <sup>3</sup> )	Frame area (cm <sup>2</sup> )
3-21-97-9	56.07	1024.00
3-21-97-9	58.39	1024.00
3-21-97-9	58.04	1024.00
3-21-97-9	56.25	1024.00
Sample No.	Closure volume (cm <sup>3</sup> )	Frame area (cm <sup>2</sup> )
3-21-97-10	129.57	1024.00
3-21-97-10	131.20	1024.00
3-21-97-10	154.70	1024.00
3-21-97-10	127.89	1024.00
Sample No.	Closure volume (cm <sup>3</sup> )	Frame area (cm <sup>2</sup> )
3-21-97-11	73.32	1024.00
3-21-97-11	74.41	1024.00
3-21-97-11	75.14	1024.00
3-21-97-11	76.77	1024.00
Sample No.	Closure volume (cm <sup>3</sup> )	Frame area (cm <sup>2</sup> )
3-21-97-12	123.25	1024.00
3-21-97-12	124.49	1024.00
3-21-97-12	126.43	1024.00
3-21-97-12	134.56	1024.00

Closure Volume Statistics						
n	Mean	Std. Dev.	Std. Error	Range	Maximum	Minimum
12	146.220	80.677	23.289	237.836	294.623	56.787
Standard Deviation Statistics						
n	Mean	Std. Dev.	Std. Error	Range	Maximum	Minimum
12	1.306	0.339	0.0979	1.120	1.920	0.800

### SITE 3 SUMMARY DATA

Location: Latitude 34°13'50", Longitude 106°59'06"

Elevation: 4650 feet

Sample No.	Closure volume (cm <sup>3</sup> )	Frame area (cm <sup>2</sup> )	Standard Deviation (%)
5-2-97-1	135.873	1024.00	1.49
5-2-97-2	152.270	1024.00	2.46
5-2-97-3	95.157	1024.00	1.32
5-2-97-4	125.827	1024.00	1.03
5-2-97-5	137.337	1024.00	0.70
5-2-97-6	116.843	1024.00	1.10
5-2-97-7	91.353	1024.00	0.62
5-2-97-8	118.150	1024.00	1.53
5-2-97-9	115.680	1024.00	1.85

Closure Volume Statistics						
Size	Mean	Std. Dev.	Std. Error	Range	Maximum	Minimum
9	120.943	19.652	6.551	60.917	152.270	91.353
Standard Deviation Statistics						
Size	Mean	Std. Dev.	Std. Error	Range	Maximum	Minimum
9	1.344	0.576	0.192	1.840	2.460	0.620

### SITE 3 Raw Data

Sample No.	Closure volume (cm <sup>3</sup> )	Frame area (cm <sup>2</sup> )
5-2-97-1	133.60	1024.00
5-2-97-1	136.56	1024.00
5-2-97-1	137.94	1024.00
5-2-97-1	137.46	1024.00
Sample No.	Closure volume (cm <sup>3</sup> )	Frame area (cm <sup>2</sup> )
5-2-97-2	197.56	1024.00
5-2-97-2	155.07	1024.00
5-2-97-2	150.44	1024.00
5-2-97-2	151.30	1024.00
Sample No.	Closure volume (cm <sup>3</sup> )	Frame area (cm <sup>2</sup> )
5-2-97-3	93.94	1024.00
5-2-97-3	96.45	1024.00
5-2-97-3	95.08	1024.00
5-2-97-3	95.84	1024.00

Sample No.	Closure volume (cm <sup>3</sup> )	Frame area (cm <sup>2</sup> )
5-2-97-4	106.98	1024.00
5-2-97-4	125.34	1024.00
5-2-97-4	127.30	1024.00
5-2-97-4	124.84	1024.00
Sample No.	Closure volume (cm <sup>3</sup> )	Frame area (cm <sup>2</sup> )
5-2-97-5	126.87	1024.00
5-2-97-5	136.76	1024.00
5-2-97-5	136.83	1024.00
5-2-97-5	138.42	1024.00
Sample No.	Closure volume (cm <sup>3</sup> )	Frame area (cm <sup>2</sup> )
5-2-97-6	92.31	1024.00
5-2-97-6	118.26	1024.00
5-2-97-6	115.74	1024.00
5-2-97-6	116.53	1024.00
Sample No.	Closure volume (cm <sup>3</sup> )	Frame area (cm <sup>2</sup> )
5-2-97-7	98.32	1024.00
5-2-97-7	91.26	1024.00
5-2-97-7	91.96	1024.00
5-2-97-7	90.84	1024.00
Sample No.	Closure volume (cm <sup>3</sup> )	Frame area (cm <sup>2</sup> )
5-2-97-8	132.17	1024.00
5-2-97-8	118.84	1024.00
5-2-97-8	119.51	1024.00
5-2-97-8	116.10	1024.00
Sample No.	Closure volume (cm <sup>3</sup> )	Frame area (cm <sup>2</sup> )
5-2-97-9	109.38	1024.00
5-2-97-9	114.20	1024.00
5-2-97-9	114.71	1024.00
5-2-97-9	118.13	1024.00



## APPENDIX C: ELEVATION MEASUREMENTS

### SITE 1

Sample No 2-21-97-1, Frame area 1024 (cm <sup>2</sup> )			
x coord. (cm)	y coord. (cm)	z coord. (cm)	corrected height (cm)
0	0	7.153	0.918
5	0	6.651	0.416
10	0	6.968	0.733
15	0	7.301	1.066
20	0	7.695	1.460
25	0	8.487	2.252
0	5	7.642	1.407
5	5	6.854	0.619
10	5	7.070	0.835
15	5	7.362	1.127
20	5	7.231	0.996
25	5	7.096	0.861
0	10	6.701	0.466
5	10	7.255	1.020
10	10	6.465	0.230
15	10	6.235	0.000
20	10	6.427	0.192
25	10	7.231	0.996
0	15	7.486	1.251
5	15	7.254	1.019
10	15	7.772	1.537
15	15	7.316	1.081
20	15	7.308	1.073
25	15	7.553	1.318
0	20	7.421	1.186
5	20	7.207	0.972
10	20	7.243	1.008
15	20	7.504	1.269
20	20	7.351	1.116
25	20	7.719	1.484
0	25	7.271	1.036
5	25	7.469	1.234
10	25	7.619	1.384
15	25	7.554	1.319
20	25	7.897	1.662
25	25	7.349	1.114

Topographic variation statistical analysis:							
n	Mean	Std Dev	Std. Error	Range	Maximum	Minimum	Me
36	1.046	0.435	0.0724	2.252	2.252	0.000	1.0
25%	75%	Sum	Sum of Squares	Confidence	Skewness	Kurtosis	
0.889	1.293	37.657	45.998	0.147	-0.172	1.407	

Sample No 2-21-97-2, Frame area 1024 (cm <sup>2</sup> )			
x coord. (cm)	y coord. (cm)	z coord. (cm)	Corrected Height (cm)
0	0	7.178	0.159
5	0	7.725	0.706
10	0	7.653	0.634
15	0	7.504	0.485
20	0	7.582	0.563
25	0	7.797	0.778
0	5	7.766	0.747
5	5	7.758	0.739
10	5	7.630	0.611
15	5	7.632	0.613
20	5	7.093	0.074
25	5	7.119	0.100
0	10	7.494	0.475
5	10	7.591	0.572
10	10	7.690	0.671
15	10	7.780	0.761
20	10	7.499	0.480
25	10	7.492	0.473
0	15	7.770	0.751
5	15	7.835	0.816
10	15	7.787	0.768
15	15	7.897	0.878
20	15	7.381	0.362
25	15	7.376	0.357
0	20	7.376	0.357
5	20	7.580	0.561
10	20	7.491	0.472
15	20	7.576	0.557
20	20	7.467	0.448
25	20	7.560	0.541
0	25	7.236	0.217
5	25	7.209	0.190
10	25	7.468	0.449
15	25	7.681	0.662
20	25	7.926	0.907
25	25	7.741	0.722

Topographic variation statistical analysis:							
n	Mean	Std Dev	Std. Error	Range	Maximum	Minimum	N
36	0.546	0.217	0.0361	0.833	0.907	0.0740	0.
25%	75%	Sum	Sum of Squares	Confidence	Skewness	Kurtosis	
0.449	0.730	19.656	12.373	0.0733	-0.539	-0.308	

Sample No 2-21-97-3, Frame area 1024 cm <sup>2</sup>			
x coord. (cm)	y coord. (cm)	z coord. (cm)	Corrected Height (cm)
0	0	7.644	0.606
5	0	7.532	0.494
10	0	7.537	0.499
15	0	7.573	0.535
20	0	7.856	0.818
25	0	7.959	0.921
0	5	7.372	0.334
5	5	7.786	0.748
10	5	7.536	0.498
15	5	7.504	0.466
20	5	7.713	0.675
25	5	7.639	0.601
0	10	7.597	0.559
5	10	7.585	0.547
10	10	7.505	0.467
15	10	7.674	0.636
20	10	7.503	0.465
25	10	7.384	0.346
0	15	7.451	0.413
5	15	7.406	0.368
10	15	7.038	0.000
15	15	7.148	0.110
20	15	7.323	0.285
25	15	7.541	0.503
0	20	7.204	0.166
5	20	7.654	0.616
10	20	7.570	0.532
15	20	7.574	0.536
20	20	7.668	0.630
25	20	7.539	0.501
0	25	7.527	0.489
5	25	7.515	0.477
10	25	7.367	0.329
15	25	7.207	0.169
20	25	7.623	0.585
25	25	7.892	0.854

Topographic variation statistical analysis:							
n	Mean	Std Dev	Std. Error	Range	Maximum	Minimum	Media
36	0.494	0.197	0.0329	0.921	0.921	0.000	0.500
25%	75%	Sum	Sum of Squares	Confidence	Skewness	Kurtosis	
0.390	0.603	17.778	10.140	0.0667	-0.307	0.670	

Sample No 2-21-97-4, Frame area 1024 cm <sup>2</sup>			
x coord. (cm)	y coord. (cm)	z coord. (cm)	Corrected Elevation (cm)
0	0	7.103	0.485
5	0	6.924	0.306
10	0	7.087	0.469
15	0	7.141	0.523
20	0	7.120	0.502
25	0	6.743	0.125
0	5	6.744	0.126
5	5	6.682	0.064
10	5	7.083	0.465
15	5	7.235	0.617
20	5	6.970	0.352
25	5	7.195	0.577
0	10	6.788	0.170
5	10	6.618	0.000
10	10	6.964	0.346
15	10	7.117	0.499
20	10	7.170	0.552
25	10	7.065	0.447
0	15	7.161	0.543
5	15	6.650	0.032
10	15	6.936	0.318
15	15	7.172	0.554
20	15	7.193	0.575
25	15	6.975	0.357
0	20	7.091	0.473
5	20	6.945	0.327
10	20	7.253	0.635
15	20	7.247	0.629
20	20	7.154	0.536
25	20	7.114	0.496
0	25	7.486	0.868
5	25	6.942	0.324
10	25	7.059	0.441
15	25	6.932	0.314
20	25	7.471	0.853
25	25	7.378	0.760

Topographic variation statistical analysis:							
n	Mean	Std Dev	Std. Error	Range	Maximum	Minimum	Median
36	0.435	0.209	0.0349	0.868	0.868	0.000	0.471
25%	75%	Sum	Sum of Squares	Confidence	Skewness	Kurtosis	
0.321	0.553	15.660	8.347	0.0709	-0.210	0.0391	

Sample No 2-21-97-4, Frame area 1024 cm <sup>2</sup>			
x coord. (cm)	y coord. (cm)	z coord. (cm)	Corrected Elevation (cm)
0	0	7.103	0.485
5	0	6.924	0.306
10	0	7.087	0.469
15	0	7.141	0.523
20	0	7.120	0.502
25	0	6.743	0.125
0	5	6.744	0.126
5	5	6.682	0.064
10	5	7.083	0.465
15	5	7.235	0.617
20	5	6.970	0.352
25	5	7.195	0.577
0	10	6.788	0.170
5	10	6.618	0.000
10	10	6.964	0.346
15	10	7.117	0.499
20	10	7.170	0.552
25	10	7.065	0.447
0	15	7.161	0.543
5	15	6.650	0.032
10	15	6.936	0.318
15	15	7.172	0.554
20	15	7.193	0.575
25	15	6.975	0.357
0	20	7.091	0.473
5	20	6.945	0.327
10	20	7.253	0.635
15	20	7.247	0.629
20	20	7.154	0.536
25	20	7.114	0.496
0	25	7.486	0.868
5	25	6.942	0.324
10	25	7.059	0.441
15	25	6.932	0.314
20	25	7.471	0.853
25	25	7.378	0.760

Topographic variation statistical analysis:							
n	Mean	Std Dev	Std. Error	Range	Maximum	Minimum	Median
36	0.435	0.209	0.0349	0.868	0.868	0.000	0.471
25%	75%	Sum	Sum of Squares	Confidence	Skewness	Kurtosis	
0.321	0.553	15.660	8.347	0.0709	-0.210	0.0391	

Sample No 2-21-97-5, Frame area 1024 cm <sup>2</sup>			
x coord. (cm)	y coord. (cm)	z coord. (cm)	Corrected Elevation (cm)
0	0	7.685	0.665
5	0	7.633	0.613
10	0	7.593	0.573
15	0	7.582	0.562
20	0	7.210	0.190
25	0	7.172	0.152
0	5	7.655	0.635
5	5	7.526	0.506
10	5	7.435	0.415
15	5	7.250	0.230
20	5	7.057	0.037
25	5	7.189	0.169
0	10	7.640	0.620
5	10	7.485	0.465
10	10	7.492	0.472
15	10	7.141	0.121
20	10	7.337	0.317
25	10	7.097	0.077
0	15	7.317	0.297
5	15	7.643	0.623
10	15	7.268	0.248
15	15	6.985	-0.035
20	15	7.073	0.053
25	15	7.202	0.182
0	20	7.333	0.313
5	20	7.419	0.399
10	20	7.269	0.249
15	20	7.032	0.012
20	20	7.162	0.142
25	20	7.020	0.000
0	25	7.661	0.641
5	25	7.378	0.358
10	25	7.382	0.362
15	25	7.173	0.153
20	25	7.171	0.151
25	25	7.081	0.061

Topographic variation statistical analysis:							
n	Mean	Std Dev	Std. Error	Range	Maximum	Minimum	Medi
36	0.341	0.216	0.0360	0.700	0.700	0.000	0.308
25%	75%	Sum	Sum of Squares	Confidence	Skewness	Kurtosis	
0.181	0.524	12.288	5.831	0.0732	0.239	-1.228	

Sample No 2-21-97-6, Frame area 1024 cm <sup>2</sup>			
x coord. (cm)	y coord. (cm)	z coord. (cm)	Corrected Height (cm)
0	0	7.106	0.670
5	0	7.006	0.570
10	0	6.689	0.253
15	0	6.921	0.485
20	0	6.521	0.085
25	0	6.536	0.100
0	5	6.659	0.223
5	5	6.843	0.407
10	5	6.679	0.243
15	5	6.675	0.239
20	5	6.699	0.263
25	5	6.436	0.000
0	10	7.577	1.141
5	10	7.332	0.896
10	10	6.715	0.279
15	10	6.705	0.269
20	10	6.942	0.506
25	10	6.671	0.235
0	15	7.418	0.982
5	15	7.084	0.648
10	15	6.949	0.513
15	15	7.114	0.678
20	15	6.879	0.443
25	15	7.003	0.567
0	20	7.286	0.850
5	20	6.981	0.545
10	20	7.144	0.708
15	20	7.161	0.725
20	20	7.133	0.697
25	20	7.049	0.613
0	25	7.347	0.911
5	25	7.221	0.785
10	25	7.354	0.918
15	25	7.128	0.692
20	25	7.054	0.618
25	25	7.548	1.112

Topographic variation statistical analysis:

n	Mean	Std Dev	Std. Error	Range	Maximum	Minimum	Med
36	0.552	0.293	0.0489	1.141	1.141	0.000	0.569
25%	75%	Sum	Sum of Squares	Confidence	Skewness	Kurtosis	
0.266	0.716	19.869	13.976	0.0992	0.0797	-0.683	

Sample No 2-21-97-7, Frame area 1024 cm <sup>2</sup>			
x coord. (cm)	y coord. (cm)	z coord. (cm)	corrected height (cm)
0.00	0.00	7.768	0.676
5	0	7.830	0.738
10	0	7.665	0.573
15	0	7.622	0.530
20	0	7.531	0.439
25	0	8.093	1.001
0	5	7.644	0.552
5	5	7.686	0.594
10	5	7.519	0.427
15	5	7.333	0.241
20	5	7.602	0.510
25	5	7.666	0.574
0	10	7.419	0.327
5	10	7.575	0.483
10	10	7.449	0.357
15	10	7.453	0.361
20	10	7.535	0.443
25	10	7.404	0.312
0	15	7.360	0.268
5	15	7.562	0.470
10	15	7.341	0.249
15	15	7.175	0.083
20	15	7.194	0.102
25	15	7.375	0.283
0	20	7.159	0.067
5	20	7.195	0.103
10	20	7.329	0.237
15	20	7.513	0.421
20	20	7.365	0.273
25	20	7.432	0.340
0	25	7.431	0.339
5	25	7.292	0.200
10	25	7.273	0.181
15	25	7.469	0.377
20	25	7.590	0.498
25	25	7.092	0.000

Topographic variation statistical analysis:

n	Mean	Std Dev	Std. Error	Range	Maximum	Minimum	M
36	0.379	0.207	0.0344	1.001	1.001	0.000	0.000
25%	75%	Sum	Sum of Squares	Confidence	Skewness	Kurtosis	
0.245	0.504	13.629	6.653	0.0699	0.606	1.102	



Sample No 2-21-97-8, Frame area 1024 cm <sup>2</sup>			
x coord. (cm)	y coord. (cm)	z coord. (cm)	corrected height (cm)
0	0	5.757	0.324
5	0	5.433	0.000
10	0	6.176	0.743
15	0	7.506	2.073
20	0	6.391	0.958
25	0	7.107	1.674
0	5	7.321	1.888
5	5	5.479	0.046
10	5	6.215	0.782
15	5	6.293	0.860
20	5	7.109	1.676
25	5	7.035	1.602
0	10	5.895	0.462
5	10	6.641	1.208
10	10	6.593	1.160
15	10	7.173	1.740
20	10	7.070	1.637
25	10	7.083	1.650
0	15	6.429	0.996
5	15	7.215	1.782
10	15	7.308	1.875
15	15	7.828	2.395
20	15	7.228	1.795
25	15	7.410	1.977
0	20	7.143	1.710
5	20	6.305	0.872
10	20	7.120	1.687
15	20	7.002	1.569
20	20	7.415	1.982
25	20	6.464	1.031
0	25	7.458	2.025
5	25	6.020	0.587
10	25	6.244	0.811
15	25	6.354	0.921
20	25	7.184	1.751
25	25	7.107	1.674

Topographic variation statistical analysis:

n	Mean	Std Dev	Std. Error	Range	Maximum	Minimum	Media
36	1.331	0.609	0.101	2.395	2.395	0.000	1.619
25%	75%	Sum	Sum of Squares	Confidence	Skewness	Kurtosis	
0.866	1.767	47.923	76.768	0.206	-0.537	-0.603	

Sample No 2-21-97-9, Frame area 1024 cm <sup>2</sup>			
x coord. (cm)	y coord. (cm)	z coord. (cm)	Corrected Height (cm)
0	0	7.072	0.00
5	0	7.171	0.10
10	0	7.353	0.28
15	0	7.638	0.57
20	0	7.752	0.68
25	0	7.706	0.63
0	5	7.378	0.31
5	5	7.372	0.30
10	5	7.610	0.54
15	5	7.728	0.66
20	5	7.694	0.62
25	5	7.520	0.45
0	10	7.374	0.30
5	10	7.401	0.33
10	10	7.553	0.48
15	10	7.420	0.35
20	10	7.632	0.56
25	10	7.623	0.55
0	15	7.199	0.13
5	15	7.461	0.39
10	15	7.303	0.23
15	15	7.214	0.14
20	15	7.827	0.76
25	15	7.620	0.55
0	20	7.257	0.19
5	20	7.305	0.23
10	20	7.263	0.19
15	20	7.570	0.50
20	20	7.563	0.49
25	20	7.676	0.60
0	25	7.312	0.24
5	25	7.305	0.23
10	25	7.264	0.19
15	25	7.868	0.80
20	25	7.672	0.60
25	25	7.246	0.17

Topographic variation statistical analysis:

n	Mean	Std Dev	Std. Error	Range	Maximum	Minimum	Median
36	0.398	0.207	0.0345	0.800	0.800	0.000	0.370
25%	75%	Sum	Sum of Squares	Confidence	Skewness	Kurtosis	
0.230	0.565	14.340	7.213	0.0701	0.0865	-1.051	

Sample No 2-21-97-10, Frame area 1024 cm <sup>2</sup>			
x coord. (cm)	y coord. (cm)	z coord. (cm)	corrected height (cm)
0	0	7.125	0.496
5	0	7.361	0.732
10	0	7.503	0.874
15	0	7.624	0.995
20	0	7.418	0.789
25	0	7.129	0.500
0	5	7.289	0.660
5	5	6.851	0.222
10	5	7.197	0.568
15	5	7.516	0.887
20	5	7.771	1.142
25	5	7.124	0.495
0	10	7.100	0.471
5	10	8.008	1.379
10	10	7.388	0.759
15	10	6.919	0.290
20	10	6.830	0.201
25	10	6.796	0.167
0	15	7.444	0.815
5	15	7.326	0.697
10	15	7.410	0.781
15	15	7.007	0.378
20	15	7.138	0.509
25	15	7.074	0.445
0	20	7.135	0.506
5	20	7.664	1.035
10	20	7.326	0.697
15	20	6.629	0.000
20	20	7.071	0.442
25	20	7.433	0.804
0	25	6.949	0.320
5	25	7.190	0.561
10	25	7.364	0.735
15	25	7.378	0.749
20	25	7.155	0.526
25	25	7.234	0.605

Topographic variation statistical analysis:							
n	Mean	Std Dev	Std. Error	Range	Maximum	Minimum	Median
36	0.618	0.285	0.0476	1.379	1.379	0.000	0.587
25%	75%	Sum	Sum of Squares	Confidence	Skewness	Kurtosis	
0.458	0.785	22.232	16.580	0.0966	0.290	0.534	

Sample No 2-21-97-11, Frame area 1024 cm <sup>2</sup>			
x coord. (cm)	y coord. (cm)	z coord. (cm)	Corrected Height (cm)
0	0	7.551	0.811
5	0	7.598	0.858
10	0	7.707	0.967
15	0	7.418	0.678
20	0	7.251	0.511
25	0	7.593	0.853
0	5	7.066	0.326
5	5	7.172	0.432
10	5	7.140	0.400
15	5	7.036	0.296
20	5	7.033	0.293
25	5	7.433	0.693
0	10	6.796	0.056
5	10	6.756	0.016
10	10	7.067	0.327
15	10	6.927	0.187
20	10	7.066	0.326
25	10	7.016	0.276
0	15	6.740	0.000
5	15	6.752	0.012
10	15	6.919	0.179
15	15	7.098	0.358
20	15	7.288	0.548
25	15	6.959	0.219
0	20	6.968	0.228
5	20	7.097	0.357
10	20	7.235	0.495
15	20	7.327	0.587
20	20	7.478	0.738
25	20	7.483	0.743
0	25	7.271	0.531
5	25	7.273	0.533
10	25	7.344	0.604
15	25	7.245	0.505
20	25	7.298	0.558
25	25	7.387	0.647

Topographic variation statistical analysis:							
n	Mean	Std Dev	Std. Error	Range	Maximum	Minimum	Median
36	0.449	0.254	0.0423	0.967	0.967	0.000	0.464
25%	75%	Sum	Sum of Squares	Confidence	Skewness	Kurtosis	
0.284	0.625	16.148	9.502	0.0860	0.0400	-0.656	

Sample No 2-21-97-12, Frame area 1024 cm <sup>2</sup>			
x coord. (cm)	y coord. (cm)	z coord. (cm)	Corrected Height (cm)
0	0	7.068	0.649
5	0	7.124	0.705
10	0	7.364	0.945
15	0	7.369	0.950
20	0	7.026	0.607
25	0	6.934	0.515
0	5	6.912	0.493
5	5	6.481	0.062
10	5	7.315	0.896
15	5	7.024	0.605
20	5	7.294	0.875
25	5	6.975	0.556
0	10	7.189	0.770
5	10	7.046	0.627
10	10	6.899	0.480
15	10	6.749	0.330
20	10	6.687	0.268
25	10	6.791	0.372
0	15	6.921	0.502
5	15	7.011	0.592
10	15	7.004	0.585
15	15	6.856	0.437
20	15	6.779	0.360
25	15	6.750	0.331
0	20	6.749	0.330
5	20	6.702	0.283
10	20	6.419	0.000
15	20	7.144	0.725
20	20	7.888	1.469
25	20	6.707	0.288
0	25	7.460	1.041
5	25	6.534	0.115
10	25	6.752	0.333
15	25	7.121	0.702
20	25	7.548	1.129
25	25	7.152	0.733

Topographic variation statistical analysis:

n	Mean	Std. Dev.	Std. Error	Range	Maximum	Minimum	Median
36	0.574	0.310	0.0516	1.469	1.469	0.000	0.571
25%	75%	Sum	Sum of Squares	Confidence	Skewness	Kurtosis	
0.332	0.729	20.660	15.216	0.105	0.609	0.803	

Sample No 2-21-97-13, Frame area 1024 cm <sup>2</sup>			
x coord. (cm)	y coord. (cm)	z coord. (cm)	Corrected Height (cm)
0	0	7.308	0.267
5	0	7.468	0.427
10	0	7.516	0.475
15	0	7.310	0.269
20	0	7.479	0.438
25	0	7.598	0.557
0	5	7.512	0.471
5	5	7.320	0.279
10	5	7.248	0.207
15	5	7.305	0.264
20	5	7.799	0.758
25	5	7.245	0.204
0	10	7.524	0.483
5	10	7.561	0.520
10	10	7.397	0.356
15	10	7.623	0.582
20	10	7.421	0.380
25	10	7.304	0.263
0	15	7.754	0.713
5	15	7.520	0.479
10	15	7.708	0.667
15	15	7.303	0.262
20	15	7.322	0.281
25	15	7.288	0.247
0	20	7.327	0.286
5	20	7.518	0.477
10	20	7.736	0.695
15	20	7.275	0.234
20	20	7.268	0.227
25	20	7.452	0.411
0	25	7.360	0.319
5	25	7.330	0.289
10	25	7.041	0.000
15	25	7.547	0.506
20	25	7.552	0.511
25	25	7.406	0.365

Topographic variation statistical analysis:

n	Mean	Std. Dev.	Std. Error	Range	Maximum	Minimum	Median
36	0.394	0.168	0.0279	0.758	0.758	0.000	0.373
25%	75%	Sum	Sum of Squares	Confidence	Skewness	Kurtosis	
0.266	0.495	14.169	6.559	0.0567	0.292	-0.0444	

Sample No 2-21-97-14, Frame area 1175.8 cm <sup>2</sup>			
x coord. (cm)	y coord. (cm)	z coord. (cm)	Corrected Height (cm)
0	0	8.703	1.722
5	0	7.705	0.724
10	0	7.204	0.223
15	0	7.385	0.404
20	0	7.614	0.633
25	0	7.768	0.787
0	5	7.971	0.990
5	5	7.726	0.745
10	5	7.192	0.211
15	5	7.283	0.302
20	5	7.399	0.418
25	5	7.984	1.003
0	10	7.758	0.777
5	10	7.816	0.835
10	10	7.501	0.520
15	10	7.048	0.067
20	10	7.602	0.621
25	10	7.151	0.170
0	15	8.057	1.076
5	15	8.470	1.489
10	15	7.432	0.451
15	15	6.981	0.000
20	15	7.778	0.797
25	15	7.664	0.683
0	20	8.325	1.344
5	20	7.860	0.879
10	20	7.760	0.779
15	20	7.513	0.532
20	20	7.055	0.074
25	20	7.651	0.670
0	25	8.244	1.263
5	25	8.041	1.060
10	25	8.091	1.110
15	25	7.566	0.585
20	25	7.235	0.254
25	25	7.639	0.658

Topographic variation statistical analysis:							
n	Mean	Std. Dev.	Std. Error	Range	Maximum	Minimum	Median
36	0.690	0.407	0.0678	1.722	1.722	0.000	0.677
25%	75%	Sum	Sum of Squares	Confidence	Skewness	Kurtosis	
0.411	0.935	24.856	22.958	0.138	0.430	0.0551	

Sample No 2-21-97-15, Frame area 1024 cm <sup>2</sup>			
x coord. (cm)	y coord. (cm)	z coord. (cm)	corrected height (cm)
0	0	7.543	0.960
5	0	7.561	0.978
10	0	7.186	0.603
15	0	7.907	1.324
20	0	7.295	0.712
25	0	7.658	1.075
0	5	7.547	0.964
5	5	7.587	1.004
10	5	7.439	0.856
15	5	7.966	1.383
20	5	7.114	0.531
25	5	7.641	1.058
0	10	7.689	1.106
5	10	7.594	1.011
10	10	7.297	0.714
15	10	6.871	0.288
20	10	6.583	0.000
25	10	7.341	0.758
0	15	6.985	0.402
5	15	7.263	0.680
10	15	7.521	0.938
15	15	7.227	0.644
20	15	7.149	0.566
25	15	7.012	0.429
0	20	7.228	0.645
5	20	7.693	1.110
10	20	7.859	1.276
15	20	7.663	1.080
20	20	7.545	0.962
25	20	7.465	0.882
0	25	7.548	0.965
5	25	7.608	1.025
10	25	7.526	0.943
15	25	7.609	1.026
20	25	7.514	0.931
25	25	7.612	1.029

Topographic variation statistical analysis:							
n	Mean	Std. Dev.	Std. Error	Range	Maximum	Minimum	Media
36	0.857	0.294	0.0490	1.383	1.383	0.000	0.952
25%	75%	Sum	Sum of Squares	Confidence	Skewness	Kurtosis	
0.663	1.027	30.858	29.472	0.0994	-0.815	0.926	



Sample No 2-21-97-16, Frame area 1024 cm <sup>2</sup>			
x coord. (cm)	y coord. (cm)	z coord. (cm)	corrected height (cm)
0	0	7.694	0.056
5	0	7.952	0.314
10	0	8.152	0.514
15	0	8.121	0.483
20	0	7.991	0.353
25	0	8.041	0.403
0	5	8.351	0.713
5	5	7.963	0.325
10	5	7.974	0.336
15	5	7.899	0.261
20	5	8.343	0.705
25	5	8.607	0.969
0	10	8.328	0.690
5	10	8.140	0.502
10	10	8.270	0.632
15	10	8.207	0.569
20	10	8.293	0.655
25	10	8.672	1.034
0	15	8.211	0.573
5	15	7.638	0.000
10	15	8.663	1.025
15	15	8.522	0.884
20	15	8.414	0.776
25	15	8.619	0.981
0	20	8.394	0.756
5	20	7.978	0.340
10	20	8.544	0.906
15	20	8.263	0.625
20	20	8.401	0.763
25	20	8.716	1.078
0	25	8.314	0.676
5	25	8.112	0.474
10	25	8.658	1.020
15	25	8.380	0.742
20	25	8.630	0.992
25	25	8.824	1.186

Topographic variation statistical analysis:							
n	Mean	Std. Dev.	Std. Error	Range	Maximum	Minimum	Median
36	0.648	0.293	0.0488	1.186	1.186	0.000	0.665
25%	75%	Sum	Sum of Squares	Confidence	Skewness	Kurtosis	
0.439	0.895	23.311	18.098	0.0991	-0.211	-0.505	

Sample No 2-21-97-17, Frame area 1024 cm <sup>2</sup>			
x coord. (cm)	y coord. (cm)	z coord. (cm)	Corrected Height (cm)
0	0	8.897	1.668
5	0	8.570	1.341
10	0	7.720	0.491
15	0	8.236	1.007
20	0	8.559	1.330
25	0	8.117	0.888
0	5	7.762	0.533
5	5	7.901	0.672
10	5	7.729	0.500
15	5	8.099	0.870
20	5	7.906	0.677
25	5	8.082	0.853
0	10	7.821	0.592
5	10	7.780	0.551
10	10	7.229	0.000
15	10	7.249	0.020
20	10	8.014	0.785
25	10	8.180	0.951
0	15	8.438	1.209
5	15	8.116	0.887
10	15	8.162	0.933
15	15	8.110	0.881
20	15	8.015	0.786
25	15	8.002	0.773
0	20	8.284	1.055
5	20	8.132	0.903
10	20	8.348	1.119
15	20	8.361	1.132
20	20	8.185	0.956
25	20	7.887	0.658
0	25	8.447	1.218
5	25	8.254	1.025
10	25	8.435	1.206
15	25	8.324	1.095
20	25	8.183	0.954
25	25	7.895	0.666

Topographic variation statistical analysis:							
n	Mean	Std. Dev.	Std. Error	Range	Maximum	Minimum	Median
36	0.866	0.336	0.0559	1.668	1.668	0.000	0.887
25%	75%	Sum	Sum of Squares	Confidence	Skewness	Kurtosis	
0.669	1.075	31.185	30.957	0.114	-0.458	1.307	

Sample No 2-21-97-18, Frame area 1024 cm <sup>2</sup>			
x coord. (cm)	y coord. (cm)	z coord. (cm)	Corrected Height (cm)
0	0	7.777	1.599
5	0	7.245	1.067
10	0	7.162	0.984
15	0	7.054	0.876
20	0	6.573	0.395
25	0	6.178	0.000
0	5	7.140	0.962
5	5	7.014	0.836
10	5	6.624	0.446
15	5	7.161	0.983
20	5	6.566	0.388
25	5	6.552	0.374
0	10	7.380	1.202
5	10	7.182	1.004
10	10	7.023	0.845
15	10	6.610	0.432
20	10	6.956	0.778
25	10	6.547	0.369
0	15	6.706	0.528
5	15	7.224	1.046
10	15	6.969	0.791
15	15	7.016	0.838
20	15	6.826	0.648
25	15	6.209	0.031
0	20	6.856	0.678
5	20	7.007	0.829
10	20	6.811	0.633
15	20	6.867	0.689
20	20	7.082	0.904
25	20	6.496	0.318
0	25	6.915	0.737
5	25	6.939	0.761
10	25	6.806	0.628
15	25	7.166	0.988
20	25	7.630	1.452
25	25	7.122	0.944

Topographic variation statistical analysis:							
n	Mean	Std. Dev.	Std. Error	Range	Maximum	Minimum	Median
36	0.750	0.342	0.0570	1.599	1.599	0.000	0.784
25%	75%	Sum	Sum of Squares	Confidence	Skewness	Kurtosis	
0.487	0.972	26.983	24.316	0.116	0.0328	0.581	

Sample No 2-21-97-19,		Frame area 1024 cm <sup>2</sup>	
x coord. (cm)	y coord. (cm)	z coord. (cm)	Corrected Height (cm)
0	0	7.095	0.488
5	0	7.326	0.719
10	0	7.431	0.824
15	0	7.408	0.801
20	0	7.633	1.026
25	0	7.627	1.020
0	5	7.326	0.719
5	5	7.451	0.844
10	5	7.589	0.982
15	5	7.358	0.751
20	5	7.309	0.702
25	5	7.123	0.516
0	10	7.533	0.926
5	10	7.254	0.647
10	10	7.142	0.535
15	10	6.925	0.318
20	10	6.713	0.106
25	10	6.607	0.000
0	15	7.289	0.682
5	15	7.208	0.601
10	15	7.311	0.704
15	15	6.935	0.328
20	15	6.658	0.051
25	15	6.759	0.152
0	20	7.458	0.851
5	20	7.833	1.226
10	20	7.764	1.157
15	20	7.912	1.305
20	20	7.202	0.595
25	20	7.588	0.981
0	25	7.381	0.774
5	25	7.571	0.964
10	25	7.825	1.218
15	25	7.547	0.940
20	25	7.076	0.469
25	25	7.174	0.567

Topographic variation statistical analysis:

n	Mean	Std. Dev.	Std. Error	Range	Maximum	Minimum	Median
36	0.708	0.329	0.0548	1.305	1.305	0.000	0.719
25%	75%	Sum	Sum of Squares	Confidence	Skewness	Kurtosis	
0.526	0.952	25.489	21.838	0.111	-0.390	-0.194	

Sample No 2-21-97-20, Frame area 1024 cm <sup>2</sup>			
x coord. (cm)	y coord. (cm)	z coord. (cm)	Corrected Height (cm)
0	0	9.083	1.338
5	0	9.080	1.335
10	0	8.930	1.185
15	0	8.435	0.690
20	0	8.258	0.513
25	0	7.745	0.000
0	5	8.811	1.066
5	5	8.623	0.878
10	5	8.792	1.047
15	5	7.952	0.207
20	5	8.114	0.369
25	5	8.238	0.493
0	10	9.214	1.469
5	10	8.558	0.813
10	10	8.030	0.285
15	10	8.416	0.671
20	10	7.922	0.177
25	10	8.531	0.786
0	15	8.830	1.085
5	15	9.038	1.293
10	15	8.529	0.784
15	15	7.852	0.107
20	15	8.065	0.320
25	15	8.091	0.346
0	20	8.736	0.991
5	20	9.094	1.349
10	20	8.108	0.363
15	20	8.366	0.621
20	20	8.379	0.634
25	20	8.052	0.307
0	25	8.911	1.166
5	25	9.102	1.357
10	25	8.698	0.953
15	25	8.474	0.729
20	25	8.452	0.707
25	25	8.174	0.429

Topographic variation statistical analysis:							
n	Mean	Std. Dev.	Std. Error	Range	Maximum	Minimum	Median
36	0.746	0.412	0.0686	1.469	1.469	0.000	0.718
25%	75%	Sum	Sum of Squares	Confidence	Skewness	Kurtosis	
0.366	1.075	26.863	25.978	0.139	0.0720	-1.093	

Sample No. 2-21-97-21, Frame area 1024 cm <sup>2</sup>			
x coord. (cm)	y coord. (cm)	z coord. (cm)	corrected height (cm)
0	0	7.232	1.01
5	0	6.757	0.54
10	0	6.471	0.25
15	0	6.922	0.70
20	0	7.432	1.21
25	0	7.775	1.55
0	5	6.691	0.47
5	5	6.743	0.52
10	5	6.601	0.38
15	5	6.759	0.54
20	5	6.744	0.52
25	5	6.583	0.36
0	10	6.884	0.66
5	10	7.049	0.83
10	10	7.156	0.94
15	10	7.353	1.13
20	10	7.666	1.45
25	10	6.677	0.46
0	15	7.225	1.00
5	15	7.067	0.85
10	15	6.801	0.58
15	15	6.883	0.66
20	15	6.221	0.00
25	15	6.647	0.43
0	20	6.949	0.73
5	20	7.428	1.21
10	20	6.650	0.43
15	20	6.926	0.71
20	20	6.309	0.09
25	20	6.634	0.41
0	25	7.425	1.20
5	25	7.468	1.25
10	25	6.746	0.53
15	25	6.883	0.66
20	25	7.136	0.92
25	25	6.895	0.67

Topographic variation statistical analysis:							
n	Mean	Std. Dev.	Std. Error	Range	Maximum	Minimum	Median
36	0.718	0.365	0.0608	1.550	1.550	0.000	0.660
25%	75%	Sum	Sum of Squares	Confidence	Skewness	Kurtosis	
0.465	0.970	25.850	23.213	0.123	0.410	-0.201	

SITE 2

Sample No. 3-21-97-1, Frame area 1024 cm <sup>2</sup>			
x coord. (cm)	y coord. (cm)	z coord. (cm)	corrected height (cm)
0	0	7.196	0.950
5	0	7.758	1.512
10	0	7.695	1.449
15	0	7.062	0.816
20	0	7.487	1.241
25	0	7.399	1.153
0	5	7.236	0.990
5	5	7.390	1.144
10	5	7.331	1.085
15	5	6.950	0.704
20	5	6.841	0.595
25	5	7.438	1.192
0	10	7.009	0.763
5	10	7.058	0.812
10	10	7.087	0.841
15	10	7.368	1.122
20	10	6.705	0.459
25	10	7.283	1.037
0	15	7.371	1.125
5	15	6.796	0.550
10	15	6.246	0.000
15	15	7.062	0.816
20	15	7.463	1.217
25	15	7.302	1.056
0	20	7.618	1.372
5	20	7.679	1.433
10	20	7.324	1.078
15	20	6.965	0.719
20	20	7.346	1.100
25	20	7.242	0.996
0	25	7.640	1.394
5	25	7.078	0.832
10	25	7.516	1.270
15	25	7.372	1.126
20	25	7.793	1.547
25	25	7.485	1.239

Topographic variation statistical analysis:							
n	Mean	Std. Dev.	Std. Error	Range	Maximum	Minimum	Median
36	1.020	0.323	0.0539	1.547	1.547	0.000	1.082
25%	75%	Sum	Sum of Squares	Confidence	Skewness	Kurtosis	
0.816	1.228	36.735	0.109	-0.866	1.501		

Sample No. 3-21-97-2, Frame area 1024 cm <sup>2</sup>			
x coord. (cm)	y coord. (cm)	z coord. (cm)	corrected height (cm)
0	0	6.035	0.000
5	0	6.580	0.545
10	0	7.170	1.135
15	0	7.739	1.704
20	0	7.075	1.040
25	0	7.972	1.937
0	5	7.017	0.982
5	5	7.138	1.103
10	5	7.167	1.132
15	5	7.037	1.002
20	5	7.716	1.681
25	5	7.335	1.300
0	10	6.181	0.146
5	10	6.372	0.337
10	10	6.729	0.694
15	10	7.263	1.228
20	10	7.779	1.744
25	10	7.781	1.746
0	15	7.560	1.525
5	15	7.811	1.776
10	15	7.002	0.967
15	15	7.532	1.497
20	15	7.489	1.454
25	15	7.264	1.229
0	20	7.134	1.099
5	20	6.713	0.678
10	20	6.956	0.921
15	20	7.761	1.726
20	20	7.908	1.873
25	20	7.396	1.361
0	25	7.231	1.196
5	25	7.039	1.004
10	25	7.214	1.179
15	25	7.170	1.135
20	25	7.197	1.162
25	25	6.899	0.864

Topographic variation statistical analysis:

n	Mean	Std. Dev.	Std. Error	Range	Maximum	Minimum	Median
36	1.169	0.467	0.0778	1.937	1.937	0.000	1.148
25%	75%	Sum	Sum of Squares	Confidence	Skewness	Kurtosis	
0.974	1.511	42.102	56.868	0.158	-0.539	0.262	



Sample No. 3-21-97-3, Frame area 1024 cm <sup>2</sup>			
x coord. (cm)	y coord. (cm)	z coord. (cm)	corrected height (cm)
0	0	7.108	0.331
5	0	7.127	0.350
10	0	7.474	0.697
15	0	7.719	0.942
20	0	7.451	0.674
25	0	7.124	0.347
0	5	6.777	0.000
5	5	7.044	0.267
10	5	7.660	0.883
15	5	7.645	0.868
20	5	7.415	0.638
25	5	7.400	0.623
0	10	7.165	0.388
5	10	7.082	0.305
10	10	7.170	0.393
15	10	7.606	0.829
20	10	7.562	0.785
25	10	7.421	0.644
0	15	7.669	0.892
5	15	7.313	0.536
10	15	7.065	0.288
15	15	7.493	0.716
20	15	7.255	0.478
25	15	7.205	0.428
0	20	8.355	1.578
5	20	8.095	1.318
10	20	7.843	1.066
15	20	7.493	0.716
20	20	7.337	0.560
25	20	7.723	0.946
0	25	7.048	0.271
5	25	7.747	0.970
10	25	8.421	1.644
15	25	8.094	1.317
20	25	7.799	1.022
25	25	7.566	0.789

Topographic variation statistical analysis:							
n	Mean	Std. Dev.	Std. Error	Range	Maximum	Minimum	Median
36	0.708	0.375	0.0625	1.644	1.644	0.000	0.686
25%	75%	Sum	Sum of Squares	Confidence	Skewness	Kurtosis	
0.391	0.917	25.499	22.989	0.127	0.658	0.356	

Sample No. 3-21-97-4, Frame area 1024 cm <sup>2</sup>			
x coord. (cm)	y coord. (cm)	z coord. (cm)	corrected height (cm)
0	0	6.919	0.191
5	0	7.717	0.989
10	0	7.100	0.372
15	0	7.353	0.625
20	0	6.728	0.000
25	0	7.061	0.333
0	5	6.851	0.123
5	5	8.145	1.417
10	5	7.822	1.094
15	5	7.368	0.640
20	5	7.125	0.397
25	5	7.308	0.580
0	10	7.499	0.771
5	10	7.799	1.071
10	10	7.673	0.945
15	10	7.160	0.432
20	10	6.852	0.124
25	10	6.854	0.126
0	15	7.502	0.774
5	15	7.282	0.554
10	15	6.975	0.247
15	15	7.025	0.297
20	15	7.499	0.771
25	15	7.024	0.296
0	20	7.752	1.024
5	20	7.256	0.528
10	20	7.527	0.799
15	20	7.465	0.737
20	20	7.491	0.763
25	20	7.547	0.819
0	25	7.375	0.647
5	25	7.175	0.447
10	25	7.361	0.633
15	25	7.653	0.925
20	25	7.673	0.945
25	25	7.561	0.833

Topographic variation statistical analysis:

n	Mean	Std. Dev.	Std. Error	Range	Maximum	Minimum	Median
36	0.619	0.330	0.0550	1.417	1.417	0.000	0.637
25%	75%	Sum	Sum of Squares	Confidence	Skewness	Kurtosis	
0.353	0.826	22.269	17.591	0.112	0.0900	-0.427	

Sample No. 3-21-97-5, Frame area 1024 cm <sup>2</sup>			
x coord. (cm)	y coord. (cm)	z coord. (cm)	corrected height (cm)
0	0	7.262	1.109
5	0	8.003	1.850
10	0	8.005	1.852
15	0	6.686	0.533
20	0	6.153	0.000
25	0	6.681	0.528
0	5	7.250	1.097
5	5	7.172	1.019
10	5	8.334	2.181
15	5	8.661	2.508
20	5	7.975	1.822
25	5	7.497	1.344
0	10	7.124	0.971
5	10	6.864	0.711
10	10	8.086	1.933
15	10	9.222	3.069
20	10	9.482	3.329
25	10	8.115	1.962
0	15	6.844	0.691
5	15	6.833	0.680
10	15	7.762	1.609
15	15	7.745	1.592
20	15	8.733	2.580
25	15	8.213	2.060
0	20	7.222	1.069
5	20	6.565	0.412
10	20	7.553	1.400
15	20	7.524	1.371
20	20	9.047	2.894
25	20	8.461	2.308
0	25	7.475	1.322
5	25	7.365	1.212
10	25	7.295	1.142
15	25	7.794	1.641
20	25	8.484	2.331
25	25	8.156	2.003

Topographic variation statistical analysis:							
n	Mean	Std. Dev.	Std. Error	Range	Maximum	Minimum	Mediar
36	1.559	0.784	0.131	3.329	3.329	0.000	1.496
25%	75%	Sum	Sum of Squares	Confidence	Skewness	Kurtosis	
1.044	2.032	56.135	109.072	0.265	0.285	-0.318	

Sample No. 3-21-97-6, Frame area 1024 cm <sup>2</sup>			
x coord. (cm)	y coord. (cm)	z coord. (cm)	Corrected Height (cm)
0	0	7.993	1.295
5	0	7.006	0.308
10	0	6.822	0.124
15	0	6.799	0.101
20	0	6.971	0.273
25	0	6.831	0.133
0	5	7.254	0.556
5	5	7.571	0.873
10	5	7.507	0.809
15	5	7.465	0.767
20	5	7.414	0.716
25	5	6.930	0.232
0	10	7.007	0.309
5	10	6.929	0.231
10	10	7.223	0.525
15	10	7.124	0.426
20	10	7.262	0.564
25	10	7.085	0.387
0	15	7.234	0.536
5	15	7.045	0.347
10	15	7.244	0.546
15	15	7.104	0.406
20	15	6.947	0.249
25	15	7.560	0.862
0	20	7.282	0.584
5	20	7.559	0.861
10	20	7.237	0.539
15	20	7.077	0.379
20	20	6.913	0.215
25	20	7.139	0.441
0	25	6.947	0.249
5	25	7.194	0.496
10	25	7.300	0.602
15	25	7.161	0.463
20	25	7.319	0.621
25	25	6.698	0.000

Topographic variation statistical analysis:							
n	Mean	Std. Dev.	Std. Error	Range	Maximum	Minimum	Median
36	0.473	0.267	0.0445	1.295	1.295	0.000	0.452
25%	75%	Sum	Sum of Squares	Confidence	Skewness	Kurtosis	
0.261	0.593	17.025	10.547	0.0904	0.789	1.192	

Sample No. 3-21-97-7, Frame area 1024 cm <sup>2</sup>			
x coord. (cm)	y coord. (cm)	z coord. (cm)	corrected height (cm)
0	0	7.664	1.541
5	0	7.307	1.184
10	0	6.859	0.736
15	0	6.926	0.803
20	0	6.776	0.653
25	0	7.239	1.116
0	5	8.066	1.943
5	5	7.751	1.628
10	5	6.216	0.093
15	5	6.123	0.000
20	5	6.861	0.738
25	5	6.636	0.513
0	10	7.420	1.297
5	10	7.217	1.094
10	10	7.693	1.570
15	10	6.981	0.858
20	10	6.297	0.174
25	10	6.457	0.334
0	15	6.948	0.825
5	15	7.310	1.187
10	15	7.158	1.035
15	15	8.047	1.924
20	15	7.294	1.171
25	15	7.521	1.398
0	20	6.974	0.851
5	20	7.306	1.183
10	20	7.602	1.479
15	20	7.301	1.178
20	20	7.292	1.169
25	20	7.650	1.527
0	25	6.978	0.855
5	25	7.523	1.400
10	25	7.803	1.680
15	25	7.784	1.661
20	25	7.492	1.369
25	25	6.998	0.875

Topographic variation statistical analysis:							
n	Mean	Std. Dev.	Std. Error	Range	Maximum	Minimum	Median
36	1.084	0.486	0.0809	1.943	1.943	0.000	1.170
25%	75%	Sum	Sum of Squares	Confidence	Skewness	Kurtosis	
0.814	1.440	39.042	50.596	0.164	-0.428	-0.166	

Sample No. 3-21-97-8, Frame area 1024 cm <sup>2</sup>			
x coord. (cm)	y coord. (cm)	z coord. (cm)	corrected height (cm)
0	0	5.757	0.324
5	0	5.433	0.000
10	0	6.176	0.743
15	0	7.506	2.073
20	0	6.391	0.958
25	0	7.107	1.674
0	5	7.321	1.888
5	5	5.479	0.046
10	5	6.215	0.782
15	5	6.293	0.860
20	5	7.109	1.676
25	5	7.035	1.602
0	10	5.895	0.462
5	10	6.641	1.208
10	10	6.593	1.160
15	10	7.173	1.740
20	10	7.070	1.637
25	10	7.083	1.650
0	15	6.429	0.996
5	15	7.215	1.782
10	15	7.308	1.875
15	15	7.828	2.395
20	15	7.228	1.795
25	15	7.410	1.977
0	20	7.143	1.710
5	20	6.305	0.872
10	20	7.120	1.687
15	20	7.002	1.569
20	20	7.415	1.982
25	20	6.464	1.031
0	25	7.458	2.025
5	25	6.020	0.587
10	25	6.244	0.811
15	25	6.354	0.921
20	25	7.184	1.751
25	25	7.107	1.674

Topographic variation statistical analysis:

n	Mean	Std. Dev.	Std. Error	Range	Maximum	Minimum	Median
36	1.331	0.609	0.101	2.395	2.395	0.000	1.619
25%	75%	Sum	Sum of Squares	Confidence	Skewness	Kurtosis	
0.866	1.767	47.923	76.768	0.206	-0.537	-0.603	

Sample No. 3-21-97-9, Frame area 1024 cm <sup>2</sup>			
x coord. (cm)	y coord. (cm)	z coord. (cm)	corrected height (cm)
0	0	7.143	1.281
5	0	6.388	0.526
10	0	6.331	0.469
15	0	6.403	0.541
20	0	6.686	0.824
25	0	6.794	0.932
0	5	7.292	1.430
5	5	7.231	1.369
10	5	6.318	0.456
15	5	6.553	0.691
20	5	6.236	0.374
25	5	7.295	1.433
0	10	7.592	1.730
5	10	7.049	1.187
10	10	6.862	1.000
15	10	6.579	0.717
20	10	6.537	0.675
25	10	6.768	0.906
0	15	7.441	1.579
5	15	7.463	1.601
10	15	6.778	0.916
15	15	7.245	1.383
20	15	5.862	0.000
25	15	6.731	0.869
0	20	7.853	1.991
5	20	7.400	1.538
10	20	7.378	1.516
15	20	6.621	0.759
20	20	6.468	0.606
25	20	6.332	0.470
0	25	7.376	1.514
5	25	8.075	2.213
10	25	7.890	2.028
15	25	7.131	1.269
20	25	7.849	1.987
25	25	7.241	1.379

Topographic variation statistical analysis:							
n	Mean	Std. Dev.	Std. Error	Range	Maximum	Minimum	Median
36	1.116	0.542	0.0904	2.213	2.213	0.000	1.094
25%	75%	Sum	Sum of Squares	Confidence	Skewness	Kurtosis	
0.683	1.515	40.159	55.086	0.183	0.134	-0.730	

Sample No. 3-21-97-10, Frame area 1024 cm <sup>2</sup>			
x coord. (cm)	y coord. (cm)	z coord. (cm)	corrected height (cm)
0	0	7.476	1.357
5	0	7.019	0.900
10	0	6.567	0.448
15	0	6.517	0.398
20	0	6.119	0.000
25	0	7.310	1.191
0	5	7.813	1.694
5	5	7.634	1.515
10	5	7.037	0.918
15	5	7.349	1.230
20	5	7.292	1.173
25	5	7.666	1.547
0	10	7.669	1.550
5	10	7.824	1.705
10	10	7.359	1.240
15	10	7.434	1.315
20	10	7.822	1.703
25	10	7.377	1.258
0	15	7.657	1.538
5	15	7.542	1.423
10	15	7.240	1.121
15	15	7.428	1.309
20	15	7.599	1.480
25	15	6.869	0.750
0	20	7.562	1.443
5	20	7.508	1.389
10	20	7.371	1.252
15	20	7.616	1.497
20	20	7.015	0.896
25	20	6.531	0.412
0	25	6.982	0.863
5	25	6.678	0.559
10	25	8.287	2.168
15	25	7.108	0.989
20	25	6.306	0.187
25	25	7.172	1.053

Topographic variation statistical analysis:							
n	Mean	Std. Dev.	Std. Error	Range	Maximum	Minimum	Median
36	1.152	0.472	0.0786	2.168	2.168	0.000	1.246
25%	75%	Sum	Sum of Squares	Confidence	Skewness	Kurtosis	
0.898	1.489	41.471	55.563	0.160	-0.585	0.242	



Sample No. 3-21-97-11, Frame area 1024 cm <sup>2</sup>			
x coord. (cm)	y coord. (cm)	z coord. (cm)	Corrected Height (cm)
0	0	6.262	0.483
5	0	5.943	0.164
10	0	6.079	0.300
15	0	5.978	0.199
20	0	6.973	1.194
25	0	7.097	1.318
0	5	6.162	0.383
5	5	6.407	0.628
10	5	6.713	0.934
15	5	6.424	0.645
20	5	6.802	1.023
25	5	7.113	1.334
0	10	5.779	0.000
5	10	6.828	1.049
10	10	6.639	0.860
15	10	6.455	0.676
20	10	6.933	1.154
25	10	7.301	1.522
0	15	5.868	0.089
5	15	6.812	1.033
10	15	7.335	1.556
15	15	6.721	0.942
20	15	6.387	0.608
25	15	6.837	1.058
0	20	7.360	1.581
5	20	6.823	1.044
10	20	6.837	1.058
15	20	7.244	1.465
20	20	7.956	2.177
25	20	7.722	1.943
0	25	6.532	0.753
5	25	7.349	1.570
10	25	7.605	1.826
15	25	7.788	2.009
20	25	7.570	1.791
25	25	6.773	0.994

Topographic variation statistical analysis:							
n	Mean	Std. Dev.	Std. Error	Range	Maximum	Minimum	Median
36	1.038	0.566	0.0943	2.177	2.177	0.000	1.039
25%	75%	Sum	Sum of Squares	Confidence	Skewness	Kurtosis	
0.637	1.494	37.363	49.993	0.192	0.0628	-0.623	

Sample No. 3-21-97-12, Frame area 1024 cm <sup>2</sup>			
x coord. (cm)	y coord. (cm)	z coord. (cm)	corrected height (cm)
0	0	7.507	1.700
5	0	7.315	1.508
10	0	7.559	1.752
15	0	6.761	0.954
20	0	5.807	0.000
25	0	6.740	0.933
0	5	6.727	0.920
5	5	6.825	1.018
10	5	6.073	0.266
15	5	6.621	0.814
20	5	6.942	1.135
25	5	5.868	0.061
0	10	5.901	0.094
5	10	6.754	0.947
10	10	7.124	1.317
15	10	7.224	1.417
20	10	7.142	1.335
25	10	6.720	0.913
0	15	7.453	1.646
5	15	7.366	1.559
10	15	7.614	1.807
15	15	7.878	2.071
20	15	7.651	1.844
25	15	7.102	1.295
0	20	7.365	1.558
5	20	7.021	1.214
10	20	8.007	2.200
15	20	7.836	2.029
20	20	7.848	2.041
25	20	7.266	1.459
0	25	6.822	1.015
5	25	7.120	1.313
10	25	7.015	1.208
15	25	7.739	1.932
20	25	7.688	1.881
25	25	7.203	1.396

Topographic variation statistical analysis:							
n	Mean	Std. Dev.	Std. Error	Range	Maximum	Minimum	Mediar
36	1.293	0.569	0.0949	2.200	2.200	0.000	1.326
25%	75%	Sum	Sum of Squares	Confidence	Skewness	Kurtosis	
0.950	1.726	46.552	71.543	0.193	-0.683	0.155	

SITE 3

Sample No. 5-2-97-1, Frame area 1024 cm <sup>2</sup>			
x coord. (cm)	y coord. (cm)	z coord. (cm)	corrected height (cm)
0	0	7.462	1.071
5	0	8.006	1.615
10	0	7.658	1.267
15	0	7.498	1.107
20	0	6.453	0.062
25	0	6.435	0.044
0	5	7.513	1.122
5	5	7.971	1.580
10	5	8.015	1.624
15	5	7.306	0.915
20	5	6.945	0.554
25	5	6.591	0.200
0	10	7.634	1.243
5	10	7.783	1.392
10	10	7.819	1.428
15	10	7.448	1.057
20	10	7.561	1.170
25	10	6.975	0.584
0	15	7.640	1.249
5	15	7.500	1.109
10	15	7.464	1.073
15	15	7.612	1.221
20	15	7.761	1.370
25	15	8.107	1.716
0	20	6.653	0.262
5	20	7.214	0.823
10	20	7.560	1.169
15	20	7.923	1.532
20	20	7.812	1.421
25	20	8.029	1.638
0	25	6.391	0.000
5	25	6.908	0.517
10	25	7.274	0.883
15	25	7.704	1.313
20	25	7.594	1.203
25	25	7.584	1.193

Topographic variation statistical analysis:							
n	Mean	Std. Dev.	Std. Error	Range	Maximum	Minimum	Medi
36	1.048	0.479	0.0799	1.716	1.716	0.000	1.170
25%	75%	Sum	Sum of Squares	Confidence	Skewness	Kurtosis	
0.853	1.381	37.727	47.575	0.162	-0.886	-0.0587	

Sample No. 5-2-97-2, Frame area 1024 cm <sup>2</sup>			
x coord. (cm)	y coord. (cm)	z coord. (cm)	corrected height (cm)
0	0	8.043	4.842
5	0	7.768	4.567
10	0	6.397	3.196
15	0	6.216	3.015
20	0	4.850	1.649
25	0	3.201	0.000
0	5	7.667	4.466
5	5	7.342	4.141
10	5	7.576	4.375
15	5	7.375	4.174
20	5	7.073	3.872
25	5	5.411	2.210
0	10	7.419	4.218
5	10	7.923	4.722
10	10	7.576	4.375
15	10	7.780	4.579
20	10	7.692	4.491
25	10	7.532	4.331
0	15	7.431	4.230
5	15	7.505	4.304
10	15	7.771	4.570
15	15	7.587	4.386
20	15	7.355	4.154
25	15	7.345	4.144
0	20	7.291	4.090
5	20	7.450	4.249
10	20	7.264	4.063
15	20	7.115	3.914
20	20	6.828	3.627
25	20	6.805	3.604
0	25	7.472	4.271
5	25	7.909	4.708
10	25	7.364	4.163
15	25	6.865	3.664
20	25	6.659	3.458
25	25	6.533	3.332

Topographic variation statistical analysis:							
n	Mean	Std. Dev.	Std. Error	Range	Maximum	Minimum	Median
36	3.893	0.945	0.158	4.842	4.842	0.000	4.168
25%	75%	Sum	Sum of Squares	Confidence	Skewness	Kurtosis	
3.646	4.380	140.154	576.925	0.320	-2.590	8.062	

Sample No. 5-2-97-3, Frame area 1024 cm <sup>2</sup>			
x coord. (cm)	y coord. (cm)	z coord. (cm)	corrected height (cm)
0	0	5.327	0.757
5	0	4.570	0.000
10	0	4.733	0.163
15	0	4.848	0.278
20	0	4.784	0.214
25	0	7.368	2.798
0	5	5.993	1.423
5	5	6.309	1.739
10	5	6.334	1.764
15	5	5.863	1.293
20	5	5.258	0.688
25	5	5.256	0.686
0	10	6.652	2.082
5	10	6.694	2.124
10	10	6.010	1.440
15	10	5.958	1.388
20	10	5.682	1.112
25	10	5.912	1.342
0	15	6.916	2.346
5	15	6.503	1.933
10	15	6.018	1.448
15	15	6.226	1.656
20	15	5.909	1.339
25	15	6.138	1.568
0	20	6.400	1.830
5	20	6.188	1.618
10	20	6.333	1.763
15	20	6.300	1.730
20	20	6.389	1.819
25	20	6.732	2.162
0	25	6.906	2.336
5	25	7.132	2.562
10	25	6.990	2.420
15	25	6.957	2.387
20	25	6.899	2.329
25	25	6.859	2.289

Topographic variation statistical analysis:							
n	Mean	Std. Dev.	Std. Error	Range	Maximum	Minimum	N
36	1.578	0.720	0.120	2.798	2.798	0.000	1.
25%	75%	Sum	Sum of Squares	Confidence	Skewness	Kurtosis	
1.316	2.143	56.826	107.832	0.244	-0.609	-0.248	

Sample No. 5-2-97-4, Frame area 1024 cm <sup>2</sup>			
x coord. (cm)	y coord. (cm)	z coord. (cm)	corrected height (cm)
0	0	7.529	1.884
5	0	7.125	1.480
10	0	6.991	1.346
15	0	7.284	1.639
20	0	6.950	1.305
25	0	7.141	1.496
0	5	7.198	1.553
5	5	7.236	1.591
10	5	7.407	1.762
15	5	7.463	1.818
20	5	7.347	1.702
25	5	7.238	1.593
0	10	6.226	0.581
5	10	7.171	1.526
10	10	7.226	1.581
15	10	7.468	1.823
20	10	7.374	1.729
25	10	7.444	1.799
0	15	5.645	0.000
5	15	6.904	1.259
10	15	7.657	2.012
15	15	7.547	1.902
20	15	7.700	2.055
25	15	7.185	1.540
0	20	6.437	0.792
5	20	6.519	0.874
10	20	7.660	2.015
15	20	7.493	1.848
20	20	7.231	1.586
25	20	6.775	1.130
0	25	7.282	1.637
5	25	6.963	1.318
10	25	6.985	1.340
15	25	7.262	1.617
20	25	7.116	1.471
25	25	7.030	1.385

Topographic variation statistical analysis:							
n	Mean	Std. Dev.	Std. Error	Range	Maximum	Minimum	Median
36	1.500	0.418	0.0697	2.055	2.055	0.000	1.583
25%	75%	Sum	Sum of Squares	Confidence	Skewness	Kurtosis	
1.343	1.781	53.989	87.095	0.142	-1.688	3.959	

Sample No. 5-2-97-5, Frame area 1024 cm <sup>2</sup>			
x coord. (cm)	y coord. (cm)	z coord. (cm)	corrected height (cm)
0	0	6.133	0.056
5	0	6.671	0.594
10	0	6.926	0.849
15	0	6.248	0.171
20	0	6.143	0.066
25	0	6.077	0.000
0	5	6.941	0.864
5	5	7.163	1.086
10	5	7.353	1.276
15	5	7.654	1.577
20	5	7.484	1.407
25	5	6.934	0.857
0	10	7.172	1.095
5	10	7.887	1.810
10	10	7.633	1.556
15	10	7.783	1.706
20	10	7.154	1.077
25	10	6.559	0.482
0	15	7.123	1.046
5	15	7.260	1.183
10	15	7.833	1.756
15	15	7.668	1.591
20	15	7.501	1.424
25	15	6.932	0.855
0	20	7.045	0.968
5	20	7.608	1.531
10	20	7.644	1.567
15	20	7.887	1.810
20	20	7.282	1.205
25	20	7.081	1.004
0	25	7.310	1.233
5	25	7.429	1.352
10	25	7.544	1.467
15	25	7.563	1.486
20	25	7.102	1.025
25	25	6.866	0.789

Topographic variation statistical analysis:							
n	Mean	Std. Dev.	Std. Error	Range	Maximum	Minimum	Median
36	1.106	0.500	0.0833	1.810	1.810	0.000	1.139
25%	75%	Sum	Sum of Squares	Confidence	Skewness	Kurtosis	
0.856	1.509	39.821	52.786	0.169	-0.746	-0.0224	

Sample No. 5-2-97-6, Frame area 1024 cm <sup>2</sup>			
x coord. (cm)	y coord. (cm)	z coord. (cm)	corrected height (cm)
0	0	7.027	1.651
5	0	6.399	1.023
10	0	5.841	0.465
15	0	5.602	0.226
20	0	5.516	0.140
25	0	5.618	0.242
0	5	6.611	1.235
5	5	5.376	0.000
10	5	5.662	0.286
15	5	5.904	0.528
20	5	5.695	0.319
25	5	5.456	0.080
0	10	5.834	0.458
5	10	6.642	1.266
10	10	5.640	0.264
15	10	5.581	0.205
20	10	5.574	0.198
25	10	5.864	0.488
0	15	6.883	1.507
5	15	6.760	1.384
10	15	6.674	1.298
15	15	5.882	0.506
20	15	6.679	1.303
25	15	5.622	0.246
0	20	6.864	1.488
5	20	7.004	1.628
10	20	6.693	1.317
15	20	6.867	1.491
20	20	6.958	1.582
25	20	6.728	1.352
0	25	6.907	1.531
5	25	6.579	1.203
10	25	7.065	1.689
15	25	6.682	1.306
20	25	7.003	1.627
25	25	6.846	1.470

Topographic variation statistical analysis:							
n	Mean	Std. Dev.	Std. Error	Range	Maximum	Minimum	Media
36	0.917	0.592	0.0986	1.689	1.689	0.000	1.219
25%	75%	Sum	Sum of Squares	Confidence	Skewness	Kurtosis	
0.275	1.479	33.002	42.509	0.200	-0.184	-1.756	



Sample No. 5-2-97-7, Frame area 1024 cm <sup>2</sup>			
x coord. (cm)	y coord. (cm)	z coord. (cm)	corrected height (cm)
0	0	6.746	2.561
5	0	6.405	2.220
10	0	6.353	2.168
15	0	6.057	1.872
20	0	6.168	1.983
25	0	6.690	2.505
0	5	6.453	2.268
5	5	6.559	2.374
10	5	6.486	2.301
15	5	6.391	2.206
20	5	4.405	0.220
25	5	6.836	2.651
0	10	6.262	2.077
5	10	6.446	2.261
10	10	6.581	2.396
15	10	6.518	2.333
20	10	6.069	1.884
25	10	7.150	2.965
0	15	6.441	2.256
5	15	6.859	2.674
10	15	7.014	2.829
15	15	6.894	2.709
20	15	7.253	3.068
25	15	7.287	3.102
0	20	5.722	1.537
5	20	6.829	2.644
10	20	6.911	2.726
15	20	6.815	2.630
20	20	7.347	3.162
25	20	6.953	2.768
0	25	4.185	0.000
5	25	4.879	0.694
10	25	6.108	1.923
15	25	5.793	1.608
20	25	6.904	2.719
25	25	7.160	2.975

Topographic variation statistical analysis:

n	Mean	Std. Dev.	Std. Error	Range	Maximum	Minimum	M
36	2.257	0.725	0.121	3.162	3.162	0.000	2.3
25%	75%	Sum	Sum of Squares	Confidence	Skewness	Kurtosis	
2.030	2.714	81.269	201.853	0.245	-1.676	3.141	

Sample No. 5-2-97-8, Frame area 1024 cm <sup>2</sup>			
x coord. (cm)	y coord. (cm)	z coord. (cm)	corrected height (cm)
0	0	6.846	0.961
5	0	6.482	0.597
10	0	6.636	0.751
15	0	6.727	0.842
20	0	6.926	1.041
25	0	7.498	1.613
0	5	6.920	1.035
5	5	7.121	1.236
10	5	7.105	1.220
15	5	6.930	1.045
20	5	7.117	1.232
25	5	6.995	1.110
0	10	7.137	1.252
5	10	7.313	1.428
10	10	7.175	1.290
15	10	6.874	0.989
20	10	6.833	0.948
25	10	6.737	0.852
0	15	6.810	0.925
5	15	6.981	1.096
10	15	6.892	1.007
15	15	7.313	1.428
20	15	7.265	1.380
25	15	6.861	0.976
0	20	6.395	0.510
5	20	6.683	0.798
10	20	6.982	1.097
15	20	7.337	1.452
20	20	7.580	1.695
25	20	7.330	1.445
0	25	5.885	0.000
5	25	6.341	0.456
10	25	6.843	0.958
15	25	6.782	0.897
20	25	7.085	1.200
25	25	7.451	1.566

Topographic variation statistical analysis:							
n	Mean	Std. Dev.	Std. Error	Range	Maximum	Minimum	Median
36	1.065	0.346	0.0577	1.695	1.695	0.000	1.043
25%	75%	Sum	Sum of Squares	Confidence	Skewness	Kurtosis	
0.911	1.271	38.328	45.001	0.117	-0.709	1.429	

Sample No. 5-2-97-9, Frame area 1024 cm <sup>2</sup>			
x coord. (cm)	y coord. (cm)	z coord. (cm)	corrected height (cm)
0	0	6.465	0.220
5	0	6.646	0.401
10	0	7.297	1.052
15	0	6.617	0.372
20	0	6.581	0.336
25	0	7.048	0.803
0	5	7.448	1.203
5	5	7.417	1.172
10	5	6.997	0.752
15	5	6.294	0.049
20	5	6.687	0.442
25	5	6.245	0.000
0	10	7.295	1.050
5	10	6.650	0.405
10	10	6.652	0.407
15	10	6.645	0.400
20	10	6.747	0.502
25	10	7.191	0.946
0	15	6.531	0.286
5	15	6.697	0.452
10	15	6.744	0.499
15	15	6.944	0.699
20	15	6.598	0.353
25	15	6.618	0.373
0	20	6.610	0.365
5	20	6.925	0.680
10	20	6.651	0.406
15	20	6.378	0.133
20	20	7.179	0.934
25	20	6.640	0.395
0	25	6.343	0.098
5	25	6.474	0.229
10	25	6.823	0.578
15	25	7.247	1.002
20	25	7.637	1.392
25	25	7.338	1.093

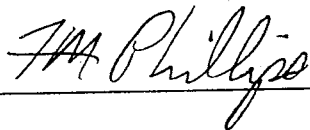
Topographic variation statistical analysis:

n	Mean	Std. Dev.	Std. Error	Range	Maximum	Minimum	Median
36	0.569	0.359	0.0598	1.392	1.392	0.000	0.424
25%	75%	Sum	Sum of Squares	Confidence	Skewness	Kurtosis	
0.359	0.869	20.479	16.162	0.121	0.596	-0.567	

This thesis is accepted on behalf of the faculty  
of the institute by the following committee:



Advisor



4/30/98  
Date